

Warm inflation model building

Mar Bastero-Gil^{1,*} and Arjun Berera^{2,†}

¹*Departamento de Física Teórica y del Cosmos, Universidad de Granada, Granada-18071, Spain*

²*School of Physics and Astronomy, University of Edinburgh, Edinburgh, EH9 3JZ, United Kingdom*

We review the main aspects of the warm inflation scenario, focusing on the inflationary dynamics and the predictions related to the primordial spectrum of perturbations, to be compared with the recent cosmological observations. We study in detail three different classes of inflationary models, chaotic, hybrid models and hilltop models, and discuss their embedding into supersymmetric models and the consequences for model building of the warm inflationary dynamics based on first principles calculations. Due to the extra friction term introduced in the inflaton background evolution generated by the dissipative dynamics, inflation can take place generically for smaller values of the field, and larger values of couplings and masses. When the dissipative dynamics dominates over the expansion, in the so-called strong dissipative regime, inflation proceeds with sub-planckian inflaton values. Models can be naturally embedded into a supergravity framework, with sugra corrections suppressed by the Planck mass now under control, for a larger class of Kähler potentials. In particular, this provides a simpler solution to the “eta” problem in supersymmetric hybrid inflation, without restricting the Kähler potentials compatible with inflation. For chaotic models dissipation leads to a smaller prediction for the tensor-to-scalar ratio and a less tilted spectrum when compared to the cold inflation scenario. We find in particular that a small component of dissipation renders the quartic model now consistent with the current CMB data.

keywords: cosmology, inflation, dissipation, fluctuation, supersymmetry.

PACS numbers: 98.80.Cq, 11.30.Pb, 12.60.Jv

Invited review for International Journal of Modern Physics A

I. INTRODUCTION

Warm inflation achieves a few milestones in the development of inflationary cosmology. First it is the only example of an inflationary dynamics in which the state of the universe during inflation is not the vacuum state, as in the standard picture, but rather an excited statistical state, with the thermal state being the one most examined. Second there are several first principles warm inflation models that by now exist, which are consistent both with cosmological observation and quantum field theory. For the standard inflation dynamics, when accounting for all aspects of the scenario up to the end of the reheating phase, there have been only a limited number of first principles models developed. Third only in warm inflation dynamics are the simplest monomial potential models consistent. Fourth, warm inflation provides an alternative solution to the graceful exit problem to the standard inflation dynamics. Finally warm inflation models are free of the “ η ”-problem, which has perplexed model building in standard inflation dynamics.

Inflation remains today the most attractive solution to the cosmological puzzles, in particular the horizon and flatness problems. To date there have been two distinct dynamical realizations of inflation. In the original picture of inflation [1, 2, 3, 4, 5], which has become the standard inflation picture, the universe rapidly supercools during inflation and subsequently a reheating phase is invoked to end inflation and put the universe back into a radiation dominated regime. This picture is termed cold, supercooled or isentropic inflation. In the other picture, termed warm or nonisentropic inflation [6], dissipative effects are important during the inflation period, so that radiation production occurs concurrently with inflationary expansion.

The idea of inflationary expansion and particle production occurring concurrently was first suggested by L.Z. Fang in his pre-inflation inflation paper in 1980 [7]. Later in the 80s, the suggestion was made by Moss [8] and Yokoyama and Maeda [9] to introduce an $\Upsilon\dot{\phi}$ term in the inflaton evolution equation, as a source of radiation production. This idea was then independently rediscovered almost a decade later by Berera and Fang [10] who went further to suggest that the dynamics of the inflaton field be governed by a Langevin equation which not only included a $\Upsilon\dot{\phi}$ dissipative term but also a noise force term that would drive the inflaton fluctuations, with a fluctuation-dissipation theorem

*Electronic address: mbg@ugr.es

†Electronic address: ab@ph.ed.ac.uk

uniquely specifying the inflaton fluctuations. Their paper established the foundations for the theory of fluctuations in warm inflation. Subsequently [6] proposed completely eliminating the reheating phase, which up to then was present in all inflation models. The new scenario was that the process of radiation production during inflation could occur under strong enough dissipation to permit a slow-roll solution within the inflationary expansion period and subsequently enough radiation could be present to end the inflation phase and smoothly enter the radiation dominated phase. This presented an alternative solution to the graceful exit problem. To complete the development of the basic warm inflation scenario, the calculations of inflaton fluctuations for an inflaton governed by a Langevin equation was done in [11].

The interesting features of the warm inflation scenario have motivated understanding the first principles origin of such a dynamics. The quantum mechanical origin of the Langevin equation for warm inflation, and the fluctuation-dissipation relation it implies were studied in [12]. The quantum field theory origin of the strong dissipation needed to realize warm inflation was first examined by Berera, Gleiser and Ramos [13]. This work proposed that solutions relevant to warm inflation should be explored within an adiabatic approximation within quantum field theory, which is the approximation that has been followed by all subsequent work in this area. Berera and Ramos [14] then proposed a two-stage interaction configuration which could yield strong dissipation as well as permit the flat potentials needed for inflation. In this model the inflaton field was directly coupled to very heavy Bose and Fermi “catalyst” fields, much heavier than the temperature scale in the universe, and these heavy fields were in turn coupled to light fields. The heaviness of the catalyst fields meant they were essentially in a zero-temperature state, and so in SUSY models the primary quantum loop corrections would cancel, thereby maintaining the flat potentials needed for inflation. Nevertheless the heavy fields acted to catalyze the production of light fields which thereby heated the universe. This two-stage mechanism alleviated concerns in realizing warm inflation from quantum field theory raised in [13] and then by Yokoyama and Linde [15]. The first calculation of dissipative coefficients for the two-stage mechanism were done by Moss and Xiong [16].

The development of a quantum field theory basis for warm inflation led to specific warm inflation models. The first model that was both consistent with cosmological constraints and quantum field theory was proposed for a case where all the fields were in a high temperature phase [17], but the model required a large number of fields and a non-standard configuration of interactions. Much more successes was obtained in implementing models with the two-stage mechanism. The first attempt at building first principles warm inflation models for common potentials such as monomial and hybrid, was done by Bastero-Gil and Berera [18]. Several such models have been developed and in this review they will be presented in detail.

There have been two earlier reviews of warm inflation. In [19] the basics of the scenario were covered and in [20] the quantum field theory dynamics was covered. In this review, the various first principles models of warm inflation that have been developed will be examined and further new analysis of these models will be done. This review is organized as follows. In Sect. II the basic warm inflation scenario is presented. In Sects. III - V first principles models of warm inflation for monomial, hybrid, and hilltop potentials respectively are examined. In Sect. VI, particle physics model building consequences of warm inflation in these models is discussed. Finally, in Sect. VII we summarize the main results and discuss future directions of development.

II. WARM INFLATION: BACKGROUND FIELD EVOLUTION

In the standard cold inflation picture, the inflaton field is taken as an isolated system, such that its potential energy density drives the quasi exponential expansion of the universe, independently of any other form of energy density which could be initially present. Indeed, any other initial component of the energy density, like radiation, will be quickly redshifted away during inflation. Under this assumption, calling $\phi(t)$ the background value of the inflaton field, with potential energy density $V(\phi)$, the inflationary evolution is given by the equation:

$$\ddot{\phi}(t) + 3H\dot{\phi}(t) + V_\phi \simeq 0, \quad (1)$$

with the expansion rate¹ $H^2 = (\dot{\phi}^2/2 + V(\phi))/(3m_P^2)$, and V_ϕ being the derivative of the potential energy with respect to the field. Inflation, i.e. accelerated expansion, happens when $\dot{\phi}^2 \ll V(\phi)$, such that $3H^2m_P^2 \simeq V(\phi)$ and $\ddot{\phi}(t) \ll H\dot{\phi}(t)$, and the equation of motion of the inflaton field reduces to:

$$3H\dot{\phi} + V_\phi \simeq 0, \quad (2)$$

¹ Throughout this article we will use the reduce Planck mass $m_P \simeq 2.4 \times 10^{18}$ GeV.

i.e., its motion is overdamped by the expansion. The consistency conditions for the approximations to hold are given by the so-called slow-roll conditions:

$$\epsilon_\phi = \frac{m_P^2}{2} \left(\frac{V_\phi}{V} \right)^2 \ll 1, \quad (3)$$

$$\eta_\phi = m_P^2 \left(\frac{V_{\phi\phi}}{V} \right) \ll 1. \quad (4)$$

Nevertheless in any particle physics realisation of the inflationary framework, the inflaton is not an isolated part of the model but it interacts with other fields. The cold inflation scenario assumes that those interactions have no effect on the inflationary dynamics and can be neglected during inflation. However, they may lead to the dissipation of the inflaton energy into other degrees of freedom, such that a small percent of the inflaton vacuum energy is transferred into other, although subdominant, kinds of energy. This is the essence of the warm inflaton scenario [6, 12, 21]. The dissipative term appears as an extra friction term in the evolution equation for the inflaton field ϕ ,

$$\ddot{\phi} + (3H + \Upsilon)\dot{\phi} + V_\phi = 0, \quad (5)$$

with Υ being the dissipative coefficient. Eq. (5) is equivalent to the evolution equation for the inflaton energy density ρ_ϕ :

$$\dot{\rho}_\phi + 3H(\rho_\phi + p_\phi) = -\Upsilon(\rho_\phi + p_\phi), \quad (6)$$

with pressure $p_\phi = \dot{\phi}^2/2 - V(\phi)$, and $\rho_\phi + p_\phi = \dot{\phi}^2$. Energy conservation then demands that the energy lost of the inflaton field must be gained by some other fluid component ρ_α , with the RHS of Eq. (6) acting as the source term:

$$\dot{\rho}_\alpha + 3H(\rho_\alpha + p_\alpha) = \Upsilon(\rho_\phi + p_\phi). \quad (7)$$

If dissipation occurs into light degrees of freedom which quickly thermalize and become radiation, then we have $\rho_\alpha = \rho_R$ and:

$$\dot{\rho}_R + 4H\rho_R = \Upsilon\dot{\phi}^2. \quad (8)$$

Radiation is not necessarily redshifted away during inflation, because it is continuously fed by the inflaton through the dissipation [21]. Inflation happens when $\rho_R \ll \rho_\phi$, but even if small when compared to the inflaton energy density it can be larger than the expansion rate with $\rho_R^{1/4} > H$. Assuming thermalization, this translates roughly into $T > H$. This is the condition for warm inflation, i.e., for the dissipation potentially affecting both the background inflaton dynamics, and the primordial spectrum of the field fluctuations. In the presence of a thermal bath, when $T > H$ the quantum fluctuations of the fields are dominated by the thermal fluctuations, with the amplitude of the super-Hubble fluctuations being dependent on T [10, 11], therefore larger than the vacuum fluctuation with an amplitude dependent only on H . Otherwise, when $T < H$ (or similarly when $\rho_R^{1/4} < H$), one just recovers the standard cold inflation scenario, where dissipation can be neglected.

During warm inflation the motion of the inflaton field has to be overdamped in order to have the accelerated expansion, but now this can be achieved due to the extra friction term Υ instead of that of the Hubble rate. And once ϕ , H , and also Υ , are in this slow-regime, the same will happen with the radiation energy density, the source term now compensating for the Hubble dilution. The equations of motion reduce then to:

$$3H(1 + Q)\dot{\phi} \simeq -V_\phi, \quad (9)$$

$$4\rho_R \simeq 3Q\dot{\phi}^2. \quad (10)$$

where we have introduced the dissipative ratio $Q = \Upsilon/(3H)$. Notice that Q is not necessarily constant. The coefficient Υ will depend on ϕ and T , and therefore depending on the model the ratio Q may increase or decrease during inflation. In the former case, the radiation density may also slowly increase. Introducing another slow-roll parameter to take into account the variation of Υ :

$$\beta_\Upsilon = m_P^2 \left(\frac{\Upsilon_\phi V_\phi}{\Upsilon V} \right), \quad (11)$$

the slow-roll conditions are now given by [22, 23, 24]:

$$\epsilon_\phi < (1 + Q), \quad \eta_\phi < (1 + Q), \quad \beta_\Upsilon < (1 + Q), \quad (12)$$

where the condition on β_Υ ensures that the variation of Υ w.r.t. ϕ is slow enough. Similarly, taking also into account the dependence on T , we have the condition:

$$\left| \frac{d \ln \Upsilon}{d \ln T} \right| < 4, \quad (13)$$

which reflects the fact that radiation has to be produced at a rate larger than the redshift due to the expansion of the universe. In addition, given that inflation may take place in the presence of a thermal bath, we have to worry about the thermal corrections to the inflaton potential not being too large, mainly that they do not induce a too large thermal mass for the inflaton. This translates into the condition:

$$\delta = \frac{TV_{T\phi}}{V_\phi} < 1. \quad (14)$$

Once the above condition is fulfilled, the slow-roll conditions in Eq. (12) ensure that Eqs. (9) and (10) hold and that ρ_R is subdominant during inflation. On the other hand, when they are not longer satisfied, either the motion is no longer overdamped and slow-roll ends, or the radiation becomes comparable to the inflaton energy density. Either way, inflation will end shortly afterwards.

Given a particular model and the dissipative coefficient Υ , we can test the viability of warm inflation scenario by integrating the slow-roll evolution equations, checking under which conditions we can get enough inflation, say among 40-60 e-folds of inflation, and checking the predictions related to the primordial spectrum. For warm inflation we need $T > H$, i.e., $\rho_R^{1/4} > H$, although with $\rho_R < \rho_\phi$. But depending on the ratio Q we can have different kind of scenarios:

(a) when $Q < 1$, dissipation is not strong enough to affect the inflaton evolution, and we recover its standard slow-roll EOM; still the thermal fluctuations of the radiation energy density will modify the field fluctuations, and affect the primordial spectrum of perturbations. This is called *weak dissipative warm inflation* (WDWI).

(b) When $Q > 1$, dissipation dominates both the background dynamics and the fluctuations, and we are in *strong dissipative warm inflation* (SDWI). Field potentials that are not flat enough to allow the standard slow-roll inflaton evolution can lead to a period of inflation due to the extra friction induced by Υ .

Given that the ratio Q will also evolve during inflation, we may have also models where we start say in WDWI but end in SDWI, or the other way round.

The main ingredient now in order to study the different possibilities is to set the functional dependence of the dissipative coefficient on ϕ and T . By now there are many phenomenological models of warm inflation [21, 22, 23, 25]. More interesting are the first principles models of warm inflation in which the dissipative coefficient Υ and effective potential are computed from quantum field theory. In particular, we will be using the near-equilibrium approximation proposed in [13] with explicit expressions for Υ developed in [16, 20]. The specific field theory models considered for the inflaton interactions leading to dissipation all follow from the two-stage mechanism in [14, 26, 27]. In this mechanism, the inflaton field ϕ is coupled to heavy Bose χ and Fermi ψ_χ ‘‘catalyst’’ fields, which in turn are coupled to light fields y_i, ψ_{y_i} . As the background inflaton field moves down the potential, it excites the heavy catalyst fields which in turn decay into light degrees of freedom [14, 26, 27, 28, 29, 30]. Consistency of the approximations then demands the microphysical dynamics determining Υ to be faster than that of the macroscopic motion of the background inflaton and the expansion [13]. Therefore, if Γ_χ is the decay width of the heavy bosonic field, we need $\Gamma_\chi > |\dot{\phi}/\phi|, H$. In addition, the condition $T \gg H$ allows to neglect the expansion of the universe when computing Υ . An important feature of such coupling configurations is that even for large perturbative couplings, in supersymmetric (susy) models, the quantum corrections to the effective potential from these terms can be controlled enough to maintain an adequately flat inflaton potential [27, 28], yet susy provides no cancellation of the time nonlocal terms, which are the dissipative terms, and so such terms can be quite significant.

We will therefore consider supersymmetric models with the interactions given in the superpotential:

$$W = W(\Phi) + g\Phi X^2 + hXY^2, \quad (15)$$

where Φ, X , and Y denote superfields. We denote by χ and y the bosonic components for X and Y respectively, but use also Φ for the inflaton scalar component when needed. The background value of the inflaton field is given then by² $\phi = \sqrt{2}\langle|\Phi|\rangle$, and we use $\delta\phi$ for its fluctuations. The full superpotential will also include the remaining interactions of X and Y with other fields. The latter are not relevant in order to compute the dominant contribution

² Without lost of generality, we will set the vev (vacuum expectation value) of the imaginary part of the inflaton field to zero.

to the dissipative coefficient, and we will not specify them. For the inflaton superpotential $W(\Phi)$ we take:

$$W(\Phi) = \frac{\lambda}{p+1} \frac{\Phi^{p+1}}{m_P^{p-2}}, \quad (16)$$

which covers the different examples given in this article: when $p > 1$ we recover the chaotic models of inflation, and with $p = 0$, $\lambda < 0$ we have the standard supersymmetric hybrid inflation. The potential is then given by:

$$V = \lambda^2 m_P^{4-2p} \left| \frac{\phi}{\sqrt{2}} + \delta\phi \right|^{2p} + 2\lambda g m_P^{2-p} \text{Re} \left[\left(\frac{\phi}{\sqrt{2}} + \delta\phi \right)^p \chi^{*2} \right] + 4g^2 \left| \frac{\phi}{\sqrt{2}} + \delta\phi \right|^2 |\chi|^2 + 4hg \text{Re} \left[\left(\frac{\phi}{\sqrt{2}} + \delta\phi \right) \chi y^{*2} \right] + g^2 |\chi|^4 + h^2 |y|^4 + 4h^2 |\chi|^2 |y|^2. \quad (17)$$

During inflation, the field y and its fermionic partner ψ_y remain massless, while the mediating field χ gets its mass from the interaction with the inflaton field ϕ , with

$$m_{\chi_R}^2 = 2g^2 \phi^2 + 2\lambda g m_P^2 \left(\frac{\phi}{\sqrt{2} m_P} \right)^p, \quad (18)$$

$$m_{\chi_I}^2 = 2g^2 \phi^2 - 2\lambda g m_P^2 \left(\frac{\phi}{\sqrt{2} m_P} \right)^p, \quad (19)$$

$$\tilde{m}_\chi^2 = 2g^2 \phi^2, \quad (20)$$

\tilde{m}_χ being the mass of the fermionic component. The bosonic interactions among χ , y and $\delta\phi$, up to second order in the inflaton fluctuations, are given by:

$$V_I = 4g^2 \frac{\phi}{\sqrt{2}} (\delta\phi + \delta\phi^*) |\chi|^2 + 4g^2 |\delta\phi|^2 |\chi|^2 + 4hg \left(\frac{\phi}{\sqrt{2}} \right) \text{Re}[\chi y^{*2}] + 4hg \text{Re}[\delta\phi \chi y^{*2}] + 2p\lambda g m_P \left(\frac{\phi}{\sqrt{2} m_P} \right)^{p-1} \text{Re}[\delta\phi \chi^{*2}] + p(p-1)\lambda g \left(\frac{\phi}{\sqrt{2} m_P} \right)^{p-2} \text{Re}[\delta\phi^2 \chi^{*2}] + \dots \quad (21)$$

Generically the inflationary constraints on the amount of inflation and the amplitude of the primordial spectrum will translate in having a small enough coupling $\lambda \ll g, h$, and $\lambda \ll \phi/m_P$, so that the terms in the second line of Eq. (21) can be neglected. The dissipative coefficient arising from this pattern of interactions among the scalar components has been computed in Ref. [16], and in particular in the low- T regime it is well approximated by:

$$\Upsilon \simeq 0.64 \times g^2 h^4 \sum_{i=R,I} \left(\frac{g\phi}{m_{\chi_i}} \right)^4 \frac{T^3}{m_{\chi_i}^2}. \quad (22)$$

The fermionic decay of the X field into the Y fermions, and/or the interaction of the field fluctuations with the X fermions, which can be found in Ref. [16], also contribute to the dissipative coefficient, but this is subdominant in the low- T regime and it can be neglected. And also in general we will have $m_{\chi_R} \simeq m_{\chi_I} \simeq m_\chi$, either due to the smallness of the coupling λ in chaotic models, or whenever we are not close to the critical value in hybrid models. The low- T approximation only applies when $T/m_\chi \lesssim 0.1$, and hereon we will restrict the analyses to this regime. The main reason is to be able to study the system analytically and get the main features of the evolution. For models where this low- T condition is violated during inflation, we need to use the exact integral expressions for the dissipative coefficient given in Ref. [16] and numerically integrate the equations. Taking into account dissipation in the intermediate/high T regime will add some extra e-folds of inflation either at the beginning or the end of the low- T regime, depending on the evolution of m_χ/T . Disregarding this contribution what we obtain is a conservative bound on the parameter models for warm inflation. On the other hand, the low- T requirement $T/m_\chi \lesssim 0.1$ together with the warm inflation condition $T/H > 1$ also guarantee that the adiabaticity condition $\Gamma_\chi > |\dot{\phi}/\phi|$, H holds in this regime. With $\Gamma_\chi \simeq h^2 m_\chi / (8\pi)$, and given that $|\dot{\phi}/\phi| \simeq H|\eta_\phi/(1+Q)|$ we have then:

$$\frac{\Gamma_\chi}{|\dot{\phi}/\phi|} > \frac{\Gamma_\chi}{H} > \left(\frac{\Gamma_\chi}{m_\chi} \right) \left(\frac{m_\chi}{T} \right) \left(\frac{T}{H} \right) > 1, \quad (23)$$

for values of the coupling $h^2 \approx O(1)$. This is the minimum requirement in order to have particle production of the light degrees of freedom. Once produced, their thermalization depends on details of their interactions with other particles, not included in the superpotential Eq. (15). We only assume that their couplings are large enough for

the thermalization to happen. Finally, the low- T condition $m_\chi > T$ helps in keeping the thermal corrections to the inflaton potential negligible [28].

The dissipative coefficient given in Eq. (22) does not depend on the coupling g in this regime, but only on h which can be rather large, $h \simeq O(1)$. The numerical coefficient in Eq. (22) was computed taking X, Y to be singlet complex fields. But in principle, they may belong to larger representations of a Grand Unification Theory (GUT) group, as it is typically assumed in susy hybrid models. This will give rise to an extra factor of $\mathcal{N} = N_\chi N_{decay}^2$ in front of the dissipative coefficient, where N_χ is the multiplicity of the X superfield, and N_{decay} counts the no. of decay channels available in X 's decays. Taking $m_\chi^2 = 2g^2\phi^2$, we have then:

$$\Upsilon \simeq C_\phi \frac{T^3}{\phi^2}, \quad (24)$$

where $C_\phi = 0.16 \times h^4 \mathcal{N}$.

Having set the functional form of dissipative coefficient, Eq. (24), we can obtain now from the slow-roll EOMs, Eqs. (9) and (10), the evolution of the inflaton field and the ratio Q . From Eq. (10) we have the relation between Q and ϕ :

$$Q^{1/3}(1+Q)^2 = 2\epsilon_\phi \left(\frac{C_\phi}{3}\right)^{1/3} \left(\frac{C_\phi}{4C_R}\right) \left(\frac{H}{\phi}\right)^{8/3} \left(\frac{m_P}{H}\right)^2 \quad (25)$$

where $C_R = \rho_R/T^4 = \pi^2 g_*/30$, with g_* being the effective number of light degrees of freedom³. And from Eqs. (25) and (9) we obtain the EOM:

$$\frac{d\phi/m_P}{dN_e} = -\left(\frac{\phi}{m_P}\right) \frac{\sigma_\phi}{(1+Q)}, \quad (26)$$

$$\frac{dQ}{dN_e} = \frac{Q}{1+7Q} (10\epsilon_\phi - 6\eta_\phi + 8\sigma_\phi), \quad (27)$$

where N_e is the no. of e-folds during inflation, and we have introduced for convenience the parameter:

$$\sigma_\phi = m_P^2 \left(\frac{V_\phi/\phi}{V}\right), \quad (28)$$

to give the variation of the inflaton field w.r.t the number of e-folds. This parameter is related to the slow-roll parameter β_Υ introduced in Eq. (11). In general for a dissipative parameter depending on the inflaton field like $\Upsilon \propto \phi^\alpha$ we have the slow-roll parameter $\beta_\Upsilon = \alpha\sigma_\phi$; and in particular for the low- T relation Eq. (24) then $\beta_\Upsilon = -2\sigma_\phi$.

Eqs. (26), (27), and (25) are valid in both, WDWI and SDWI, and can give the transition from one to another regime during inflation. Similarly, we can get the evolution equation for the ratio T/H , given by:

$$\frac{d \ln T/H}{dN_e} = \frac{2}{1+7Q} \left(\frac{2+4Q}{1+Q} \epsilon_\phi - \eta_\phi + \frac{1-Q}{1+Q} \sigma_\phi \right), \quad (29)$$

When $T > H$, the dominant contribution to the field spectrum are the thermal fluctuations due to the radiation, and the amplitude of the primordial spectrum is given by [10, 11, 23]:

$$P_{\mathcal{R}}^{1/2} \simeq \left| \frac{H}{\dot{\phi}} \right| P_\phi^{1/2} \simeq \left(\frac{H}{2\pi} \right) \left(\frac{3H^2}{V_\phi} \right) (1+Q)^{5/4} \left(\frac{T}{H} \right)^{1/2}, \quad (30)$$

where we have chosen to normalize the amplitude such that we recover the CI value when $Q \rightarrow 0$ and $T/H \rightarrow 1$. Using now Eqs. (26) and (27) one can derive the prediction for the spectral index:

$$n_S - 1 \simeq \frac{d \ln P_{\mathcal{R}}}{d \ln k} \simeq \frac{d P_{\mathcal{R}}}{d N_e} \simeq \frac{1}{1+Q} (- (2 - 5A_Q)\epsilon_\phi - 3A_Q\eta_\phi + (2 + 4A_Q)\sigma_\phi), \quad (31)$$

³ The different predictions and the parameter space available for warm inflation depend only mildly on g_* , and therefore we will take in the following the Minimal Supersymmetric Standard Model value $g_* \simeq 228.75$.

where

$$A_Q = \frac{Q}{1+7Q}. \quad (32)$$

The above expression for the spectral index agrees with that given in Ref. [24], Eq. (36), by replacing into their expression $b = 0$ (no thermal corrections to the inflaton potential), and $c = 3$, $\beta_{\Upsilon} = -2\sigma_\phi$, the corresponding values for the low- T dissipative coefficient Eq. (24).

For the running of the spectral index we obtain:

$$\begin{aligned} n'_S = & (1 - n_S) \frac{Q'}{1+Q} + \frac{1}{1+Q} \left(-(2 - 5A_Q)\epsilon'_\phi - 3A_Q\eta'_\phi + (2 + 4A_Q)\sigma'_\phi \right) \\ & + \frac{Q'}{(1+Q)(1+7Q)^2} (5\epsilon_\phi - 3\eta_\phi + 4\sigma_\phi), \end{aligned} \quad (33)$$

where “prime” denotes the derivative with respect to the no. of e-folds, and

$$\epsilon'_\phi = \frac{2\epsilon_\phi}{1+Q} (2\epsilon_\phi - \eta_\phi), \quad (34)$$

$$\eta'_\phi = \frac{\epsilon_\phi}{1+Q} (2\eta_\phi - \xi_\phi), \quad (35)$$

$$\sigma'_\phi = \frac{\sigma_\phi}{1+Q} (\sigma_\phi + 2\epsilon_\phi - \eta_\phi), \quad (36)$$

where $\xi_\phi = 2m_P^2(V_{\phi\phi\phi}/V_\phi)$.

Although tensor perturbations are not affected by dissipation, the ratio r of the tensor-to-scalar perturbations will change due to the modified amplitude of the primordial scalar spectrum, and we now have:

$$r \simeq \left(\frac{H}{T} \right) \frac{16\epsilon_\phi}{(1+Q)^{5/2}}, \quad (37)$$

which is suppressed w.r.t. the CI prediction by a factor $(T/H)(1+Q)^{5/2} > 1$.

On the contrary, non-gaussian effects during warm inflation [31, 32, 33] can be rather large when compared to the prediction in single field cold inflation models, which generally yield a very low value of $f_{NL} \propto n_S - 1 \lesssim 1$ [34, 35]; f_{NL} is the non-linearity parameter, defined by [36]:

$$\Phi = \Phi_L + f_{NL}\Phi_L^2, \quad (38)$$

where Φ is the curvature perturbation during the matter era, and Φ_L is its linear part. In the strong dissipative regime it was shown in [33] that entropy fluctuations during warm inflation due to the thermal fluctuations play an important role in generating large non-gaussian effects, with the prediction:

$$-15 \ln\left(1 + \frac{Q}{14}\right) - \frac{5}{2} \lesssim f_{NL} \lesssim \frac{33}{2} \ln\left(1 + \frac{Q}{14}\right) - \frac{5}{2}, \quad (39)$$

which for a dissipative ratio Q in the range from 10 to 10^6 gives that $|f_{NL}|$ ranges from 10 to 180. On the other hand, the third year WMAP CMB data [37] gives $26.9 < f_{NL} < 146.7$ at 95% confidence level, although the five year WMAP [36] data gives $-9 < f_{NL} < 111$ (95 % CL). There seems to be a tendency for $f_{NL} > 0$ in the latest data, although this still will need to be confirmed by future data, and in particular by data from Planck surveyor satellite [38]. Nevertheless, a large positive value for f_{NL} would disfavour conventional cold inflation models, whereas the strong dissipative regime could accommodate a large non-gaussian signal. And in particular the current upper bound $f_{NL} < 110$ translates into an upper bound for the dissipative ratio $Q \lesssim 1.3 \times 10^4$, and therefore on an upper bound on the dissipative parameter C_ϕ for each model.

In table I we summarize the expressions for the spectral index, running of the spectral index, and tensor-to-scalar ratio r , in the WDWI limit ($Q \ll 1$) and SDWI one ($Q \gg 1$), including also the CI limit for comparison. We notice again that these expressions hold for a dissipative coefficient that depend on T and ϕ like $\Upsilon \propto T^3/\phi^2$.

In the next sections we will particularize these predictions to the study of some simple models of inflation: (a) monomial potentials, or chaotic inflation; (b) hybrid like potentials; (c) hilltop quadratic potential. The first two kind of models have been studied in Ref. [18], and we extend those results here, whereas hilltop warm inflation was studied in [39]. We assume that the inflationary dynamics is driven by a single field, the inflaton, and that the

	$n_S - 1$	n'_S	r
CI	$2\eta_\phi - 6\epsilon_\phi$	$2\eta'_\phi - 6\epsilon'_\phi$	$16\epsilon_\phi$
WDWI	$2\sigma_\phi - 2\epsilon_\phi$	$2\sigma'_\phi - 2\epsilon'_\phi$	$16\frac{H}{T}\epsilon_\phi$
SDWI	$\frac{1}{7Q}(-3\eta_\phi + 18\sigma_\phi - 9\epsilon_\phi)$	$\frac{3}{7Q}(-\eta'_\phi + 6\sigma'_\phi - 3\epsilon'_\phi)$ $+(1 - n_S)\frac{Q'}{Q}$	$16\frac{H}{T}\frac{\epsilon_\phi}{Q^{5/2}}$

TABLE I: Predictions for the spectral index n_S , running of the spectral index n'_S and tensor-to-scalar ratio in terms of the slow-roll parameters for cold inflation (CI), and weak dissipative warm inflation (WDWI), and strong dissipative warm inflation (SDWI).

curvature perturbation is originated by its fluctuations. Using C_ϕ as a parameter, we search the parameter space available for each model to realise warm inflation, and give the predictions for the spectral index, running of the spectral index and the tensor-to-scalar ratio. The WMAP data [36] combined with the BAO and SN data indicates that $n_S = 0.96 \pm 0.013$ at the 1σ confidence level when no tensors and no running is taken into account. Allowing r and n'_S to be free parameters one has $n_S = 1.089^{+0.070}_{-0.068}$. The upper limit on the tensor-to-scalar ratio is $r < 0.22$ at the 2σ level with no running, and $r < 0.55$ when the running is included ($r < 0.4$ from [40]). For the running of the spectral index one has $n'_S = -0.053 \pm 0.028$.

III. WARM INFLATION WITH MONOMIAL POTENTIALS

We consider in this section a general chaotic inflaton potential [5] like:

$$V = V_0 \left(\frac{\phi}{m_P} \right)^n, \quad (40)$$

with $n > 0$. In a supersymmetric theory this kind of potentials can be derived from the superpotential Eq. (16), with $n = 2p$ and $V_0 = \lambda^2 m_P^4/4$. The slow-roll parameters are given by:

$$\eta_\phi = n(n-1) \left(\frac{m_P}{\phi} \right)^2, \quad \epsilon_\phi = \frac{n}{2(n-1)} \eta_\phi, \quad \sigma_\phi = \frac{\eta_\phi}{(n-1)}. \quad (41)$$

Therefore without enough dissipation, either for cold inflation with $Q = 0$ or in the weak dissipative regime with $Q \ll 1$, these potentials leads to inflation only for values of the inflaton field larger than the Planck mass m_P . Inflation ends in this case when the slow-roll conditions are no longer fulfilled, i.e., when $\eta_\phi \simeq 1$ and then $\phi_{end} \simeq \sqrt{n(n-1)}m_P$, therefore the value of the field at horizon crossing N_e e-folds before the end is given by:

$$\frac{\phi_*}{m_P} \simeq \sqrt{n(2N_e + n - 1)} \simeq \sqrt{2nN_e}. \quad (42)$$

for a total number of N_e e-folds of either CI or WDWI. For CI, the predictions for the spectral index, the running of the spectral index, and the tensor-to-scalar ratio are given by:

$$n_S \simeq 1 - \frac{2+n}{2N_e}, \quad n'_S \simeq -\frac{2+n}{2N_e^2}, \quad r \simeq \frac{4n}{N_e}, \quad (43)$$

where N_e is in the range 40 – 60. The amplitude of the scalar primordial spectrum sets the value of V_0 :

$$\frac{V_0}{m_P^4} \simeq \frac{12\pi^2 P_{\mathcal{R}}}{(2nN_e)^{n/2+1}}. \quad (44)$$

For warm inflation, the predictions will depend on the value of the coefficient C_ϕ , i.e., on whether we have enough dissipation at least to keep the ratio $T/H > 1$. The inflaton field always decreases during inflation, and the evolution of Q , Eq. (27), is given now by:

$$\frac{dQ}{dN_e} = \frac{Q}{1+7Q} \frac{(14-n)}{(n-1)} \eta_\phi, \quad (45)$$

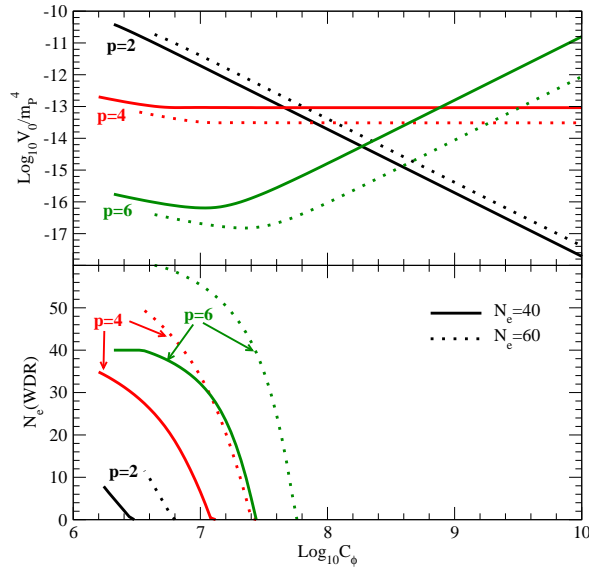


FIG. 1: Top panel: Value of V_0/m_P^4 required to match the amplitude of the primordial spectrum depending on C_ϕ , i.e., the dissipative parameter, for a monomial potential Eq. (40) with $n = 2, 4, 6$, and two choices of the total no. of e-folds since horizon crossing, $N_e = 40$ (solid lines), and $N_e = 60$ (dotted lines). Lower panel: no. of e-folds in WDWI, i.e., while $Q < 1$.

and therefore the dissipative ratio increases unless $n > 14$. Similarly, we have:

$$\left(\frac{T}{H}\right)^3 = \frac{9Q}{C_\phi} \left(\frac{m_P^4}{V_0}\right) \left(\frac{m_P}{\phi}\right)^{n-2}, \quad (46)$$

and for $n \geq 2$ the ratio T/H also increases during inflation, and thus it is enough to check for the consistency of the scenario that this ratio is larger than one only at the beginning. The other condition we need to cross-check is the low- T approximation $m_\chi/T = \sqrt{2}g\phi/T \gtrsim 10$. Given that this is the only ratio that depends on the coupling g , instead of varying this parameter we will impose this condition by taking $g \sim O(1)$ and then simply $\phi/T \gtrsim 10$, and check afterwards the constraint on the coupling g , i.e., how small the coupling can be for the results to hold. Using Eqs. (26) and (27) we have that the ratio ϕ/T evolves like:

$$\frac{d \ln \phi/T}{dN_e} = \frac{1}{1+Q} \frac{\eta_\phi}{2(n-1)} \left(n - 10 - \frac{4Q}{1+7Q}(14-n) \right), \quad (47)$$

so that in WDWI with $Q \ll 1$ this ratio decreases for $n < 10$, and in SDWI it does decrease for $n < 5$. However we have checked that as far as we fulfil the other constraints, this ratio is always larger than 10. And for the results shown in Figs. (1) and (2) we have then that the low- T condition $m_\chi/T \gtrsim 10$ holds for $n = 2$ with $g \gtrsim 0.01$, for $n = 4$ with $g \gtrsim 10^{-4}$, and for $n = 6$ with $g \gtrsim 4 \times 10^{-5}$.

The slow-roll parameter $\eta_\phi/(1+Q)$ evolves like:

$$\frac{d}{dN_e} \left(\frac{\eta_\phi}{1+Q} \right) = \left(\frac{\eta_\phi}{1+Q} \right)^2 \left(\frac{2+Qn}{1+7Q} \right) \frac{1}{n-1}, \quad (48)$$

and therefore it increases during both WD and SD warm inflation. Consequently, similarly to CI, inflation ends when $\eta_\phi = 1 + Q_f$, with Q_f being the value at the end. We remark that the slow-roll conditions are always violated before the energy density in radiation dominates. Using Eqs. (25) (see below Eq. (50)) and (46) we have the relation:

$$\frac{\eta_\phi}{1+Q} = \left(\frac{4(n-1)}{n} \right) \left(\frac{\rho_R}{V} \right) \left(\frac{1+Q}{Q} \right), \quad (49)$$

so that even when $Q_f \gg 1$ we still have $\rho_R \lesssim V$.

The procedure to get the predictions for the spectral index, ratio r and the running of the spectral index is as follows: given the value of Q_f , for each value of C_ϕ we can integrate Eq. (27) back N_e e-folds in order to get the value of the dissipative ratio at horizon crossing Q_* ; the value of V_0 is derived by matching the amplitude of the

primordial spectrum with the observational value $P_{\mathcal{R}}^{1/2} \simeq 5 \times 10^{-5}$ [36]. Mainly we are tracing the time evolution during inflation in terms of the the dissipative ratio Q , getting afterwards the value of ϕ from Eq. (25), which for monomial potentials is given by:

$$Q^{1/3}(1+Q)^2 = n^2 \left(\frac{C_\phi}{3}\right)^{1/3} \left(\frac{C_\phi}{4C_R}\right) \left(\frac{V_0}{3m_P^4}\right)^{1/3} \left(\frac{m_P}{\phi}\right)^{(14-n)/3}. \quad (50)$$

The evolution Eq. for Q is then:

$$\frac{dQ}{dN_e} = C_Q \frac{Q^{1+2s}(1+Q)^{12s}}{1+7Q}, \quad (51)$$

with

$$C_Q = n(14-n) \left(\frac{3^{1/3} 2}{D_Q n^2}\right)^{6s} \left(\frac{V_0}{m_P^4}\right)^{2s}, \quad (52)$$

$$s = \frac{1}{14-n}, \quad (53)$$

And the amplitude of the spectrum reads in this case:

$$P_{\mathcal{R}}^{1/2} = C_P Q_*^{(2-n)s/n} (1+Q_*)^{(38-13n)s/4}, \quad (54)$$

$$C_P = \frac{1}{2\pi} (3p^6 C_\phi)^{(n-2)s/2} \left(\frac{C_\phi}{12C_R}\right)^{(4+n)s} \left(\frac{V_0}{m_P^4}\right)^{6s}. \quad (55)$$

Depending on the value of C_ϕ , we can have different scenarios with: (i) N_e e-folds in WDWI, i.e., $Q_*, Q_f < 1$; (ii) $Q_* > 1$ already at N_e , i.e., SDWI; (iii) a transition after some e-folds from WDWI to SDWI, starting with $Q_* < 1$ but with $Q_f > 1$. In terms of the values for ϕ_*/m_P and Q_* , the expressions for the spectral index and the running of the spectral index, for a general power n , are given in table II, where we also include those from CI for comparison. The tilt in the spectrum and the running are also negative for warm inflation with $n > 2$, although the tilt is smaller. However for a quadratic potential with $n = 2$, when horizon crossing takes place well in WDWI with $Q_* \ll 1$, at first order in the slow-roll parameters one has a scale-invariant spectrum with no tilt and no running. Although this would be modified when including higher order corrections in the slow-roll parameters. In SDWI on the contrary, for a quadratic potential we have a blue-tilted spectrum with positive running.

Nevertheless, unless $n > 6$, we do not get 40-60 e-folds only in WDWI. Depending on the value of the parameter C_ϕ , for the smaller values inflation begins in WDWI, but after some e-folds, as Q increases, it enters into SDWI where inflation ends. This can be seen in the lower panel of Fig. (1), where is plotted the no. of e-folds of expansion in WDWI since horizon crossing, assuming that the total no. of e-folds is either 40 (solid line) or 60 (dotted line). On the top panel we have included the value of V_0 in units of m_P^4 required to get the amplitude of the primordial spectrum, i.e., the value of the coupling λ . For example for $n = 2$ this coupling is below 10^{-5} , decreasing when increasing C_ϕ ; while for $n = 4$ is rather constant with C_ϕ and of the order of 6×10^{-7} . Therefore, as mentioned in the previous section, unless the coupling g is also that small, the bosonic interactions induced by λ gives a negligible contribution to the dissipative coefficient.

	$n_S - 1$	n'_S
CI	$-n(n+2) \left(\frac{m_P}{\phi_*}\right)^2$	$-2n^2(n+2) \left(\frac{m_P}{\phi_*}\right)^4$
WDWI	$-n(n-2) \left(\frac{m_P}{\phi_*}\right)^2$	$-2n^2(n-2) \left(\frac{m_P}{\phi_*}\right)^4$
SDWI	$\frac{3}{14Q_*}(14-5n) \left(\frac{m_P}{\phi_*}\right)^2$	$\frac{3n^3}{98Q_*^2}(14-5n) \left(\frac{m_P}{\phi_*}\right)^4$

TABLE II: Predictions for the spectral index n_S and running of the spectral index n'_S for monomial potentials Eq. (40), for cold inflation (CI), weak dissipative warm inflation (WDWI), and strong dissipative warm inflation (SDWI).

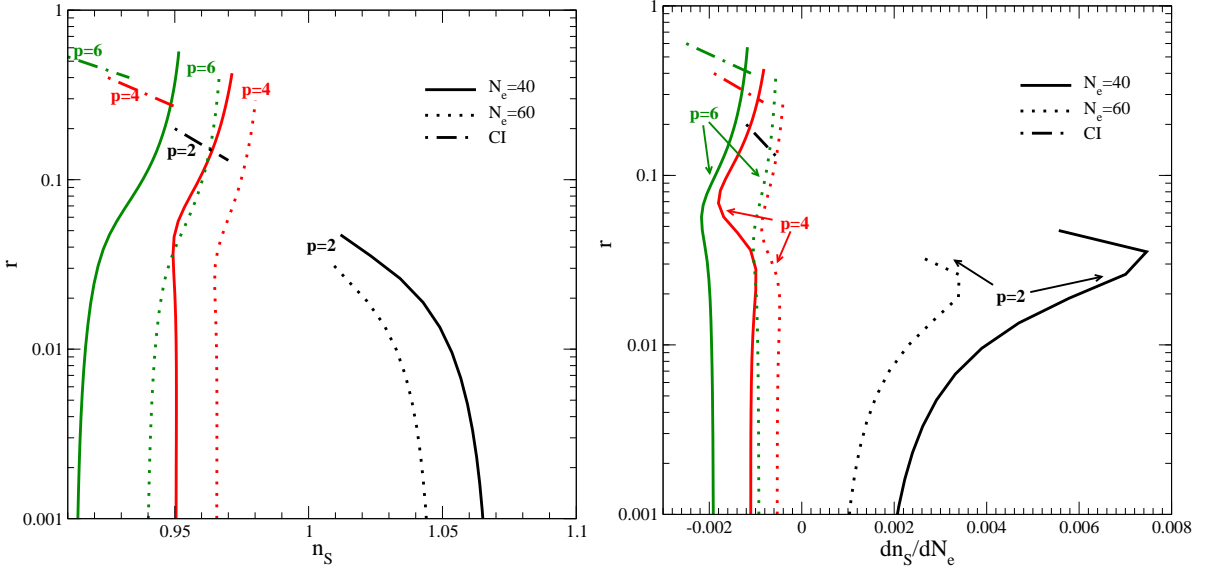


FIG. 2: LHS plot: prediction of the tensor-to-scalar r ratio versus the spectral index n_s , for monomial potentials Eq. (40) with $n = 2, 4, 6$, and two choices of the total no. of e-folds since horizon crossing, $N_e = 40$ (solid lines), and $N_e = 60$ (dotted lines). RHS plot: prediction of the running of the spectral index n'_s . The CI predictions (dashed lines) are also included for comparison.

The lower limit on C_ϕ is given by the condition $T/H \geq 1$, with Q_* and V_0 consistent with the amplitude of the primordial spectrum. The upper limit would be given by demanding not to exceed the current limit on non-gaussianity, i.e. $|f_{NL}| < 110$, which gives $Q_* < 1.3 \times 10^4$. The latter translates into $C_\phi \lesssim 2.5 \times 10^8$ (5.2×10^8) for $n = 2$ and $N_e = 40$ (60), $C_\phi \lesssim 1.1 \times 10^9$ (2.3×10^9) for $n = 4$, and $C_\phi \lesssim 2.5 \times 10^9$ (5.2×10^9) for $n = 6$. The dependence on C_ϕ for the different parameters and predictions is summarized in Table III.

The predictions for the spectral index, running and tensor-to-scalar ratio are given in Fig. (2). We have also included for comparison the predictions obtained in CI when varying the no. of e-folds between 40 and 60 (dashed lines). Well into WDWI, or SDWI, the spectral index and the running do not depend on the parameter C_ϕ , while r quickly decreases with C_ϕ : in WDWI this is due to the increasing factor T/H , and in SDWI we have also the effect of Q_* which makes the tensor contribution negligible with respect to the scalar one. Typically for warm inflation the spectrum is less tilted compared to the cold inflation scenario (and for $n = 2$ is blue-tilted), and the running is slightly larger. These two effects, the decrease in both r and the tilt of the spectrum, makes now *the quartic potential compatible with observations* [36, 40] even having only weak dissipation at horizon crossing. For example with $C_\phi \sim 6 \times 10^6$ we have $n_s \simeq 0.96$ (0.98) and $r \simeq 0.13$ (0.235) for $N_e = 40$ (60); while in CI we have $n_s \simeq 0.925$ (0.95) and $r \simeq 0.4$ (0.27), values that seem disfavoured by the latest data [36, 40]. Similarly for $p = 6$, as can be seen in Fig. (2). On the other hand, by increasing the value of the dissipative parameter C_ϕ , inflation takes place in SDWI, the tensors are negligible, and the value of the inflaton field at horizon crossing decreases *below the Planck mass*. For $p = 2$ this happens with $C_\phi \gtrsim 10^7$ (2.7×10^7) and $Q_* \gtrsim 20$ (35) for $N_e = 40$ (60); for $p = 4$ we have $C_\phi \gtrsim 9.1 \times 10^7$ (2.3×10^8) and $Q_* \gtrsim 94$ (137); and for $p = 6$ we have $C_\phi \gtrsim 3.3 \times 10^8$ (7.6×10^8) and $Q_* \gtrsim 234$ (282).

	V_0/m_P^4	ϕ_*/m_P	Q_*	$n_s - 1$	n'_s	r
WDWI	$\propto C_\phi^{-1}$	$\propto C_\phi^0$	$\propto C_\phi^3$	$\propto C_\phi^0$	$\propto C_\phi^0$	$\propto C_\phi^{-3}$
SDWI	$\propto C_\phi^{4-n}$	$\propto C_\phi^{-1}$	$\propto C_\phi^2$	$\propto C_\phi^0$	$\propto C_\phi^0$	$\propto C_\phi^{-7}$

TABLE III: Dependence on the parameter C_ϕ , for weak dissipative warm inflation (WDWI), and strong dissipative warm inflation (SDWI) for monomial potentials Eq. (40).

IV. HYBRID MODELS

We consider now small field models of inflation, with an inflationary potential given by:

$$V = V_0 \left(1 + \frac{\gamma}{n} \left(\frac{\phi}{m_P} \right)^n \right), \quad (56)$$

in general for $n > 0$, and a logarithmic potential for $n = 0$:

$$V = V_0 \left(1 + \gamma \ln \frac{\phi}{m_P} \right). \quad (57)$$

The above potentials can be regarded as the inflationary part of the supersymmetric hybrid potential derived from Eq.(16) with $p = 0$ and $\lambda < 0$, such that $V_0 = \lambda^2 m_P^4$. At tree-level the inflationary potential is a flat potential given by V_0 , but lifted either by the logarithmic radiative corrections due to the mass splitting in the X superfield, as in Eq. (57), or by the soft susy breaking mass term contributions, like in Eq. (56) with $n = 2$. In the former case we have $\gamma = g^2 N_\chi / (8\pi^2)$, N_χ being the multiplicity of X , while for the quadratic potential we have simply $\gamma = m_\phi^2 m_P^2 / V_0 = \eta_\phi$, m_ϕ being the inflaton mass. By lifting the potential by adding non-renormalizable interactions, or taking into account supergravity (sugra) corrections coming from the Kähler potential [41, 42, 43], we can also have Eq. (56) with $n \geq 2$. In general in supersymmetric models we may have all kind of lifting terms in the potential, starting with the log term from the radiative corrections, the quadratic mass from the soft susy breaking and/or sugra, and higher powers from sugra or non-renormalizable terms, and depending on the scale of inflation and the values of the couplings the dominant term can change as inflation proceeds. As we are mainly interested on the impact of the dissipative dynamics on the inflationary predictions, we will restrict the analyses in this section to the case when only one possible contribution dominates, in particular to the cases $n = 0, 2$, but this can be easily generalised to higher powers.

The total energy density during inflation is dominated anyway by the vacuum potential energy V_0 , such that H practically remains constant during inflation. But once the inflaton reaches the critical value for which the χ_R squared mass (Eq. (18)) becomes negative, the tachyonic instability in the χ field will drive the system towards the global minimum of the potential with $\langle \chi \rangle \neq 0$ and $\phi = 0$ [44, 45, 46]. Inflation may last at most until the field reaches the critical value, or may end before when the slow-roll conditions are no longer fulfilled. The slow-roll parameters are given by:

$$\eta_\phi = (n-1)\gamma \left(\frac{m_P}{\phi} \right)^{(2-n)}, \quad \epsilon_\phi = \frac{\gamma^2}{2} \left(\frac{m_P}{\phi} \right)^{(2-2n)}, \quad \sigma_\phi = \frac{\eta_\phi}{(n-1)}. \quad (58)$$

Inflation can take place for small field values with $\phi < m_P$ as far as γ is small enough. And once dissipation is taken into account, this can be the case even for values of γ larger than unity but with $\gamma/(1+Q) \ll 1$. When the potential is lifted by a mass correction, this means in particular that with dissipation a mass term larger than the Hubble scale can be compatible with inflation. Such contributions can arise in sugra models when taking into account the corrections from the Kähler potential, the so-called ‘‘eta’’ problem in sugra inflation [47]. The problem can be overcome by considering some specific forms of the Kähler potential which lead to the cancellation of the quadratic term in the potential, like in the standard susy hybrid inflationary model with minimal Kähler potential [44, 46] or by working with no-scale Kähler potentials [48, 49]; another alternative would be considering D-term inflation models [50], for which the vacuum energy originated in the potential D-term instead of the superpotential. Warm inflation provides therefore a different solution to the problem, relying on the interactions of the inflaton field but without restricting the origin of the vacuum energy and/or the kind of sugra embedding.

The slow-roll equations of motion for warm inflation read:

$$\frac{d \ln \phi / m_P}{dN_e} = -\frac{\gamma}{1+Q} \left(\frac{\phi}{m_P} \right)^{n-2}, \quad (59)$$

$$\frac{d \ln Q}{dN_e} = \frac{\gamma}{1+7Q} \left(\frac{\phi}{m_P} \right)^{n-2} \left(14 - 6n + 5\gamma \left(\frac{\phi}{m_P} \right)^n \right), \quad (60)$$

$$\frac{d \ln T/H}{dN_e} = \frac{2\gamma}{1+7Q} \left(\frac{\phi}{m_P} \right)^{n-2} \left(\frac{2}{1+Q} - n + \gamma \frac{1+2Q}{1+Q} \left(\frac{\phi}{m_P} \right)^n \right), \quad (61)$$

$$\frac{d \ln \phi/T}{dN_e} = -\frac{\gamma}{1+Q} \left(\frac{\phi}{m_P} \right)^{n-2} \left(1 + \frac{2}{1+7Q} (2 - n(1+Q)) + \frac{\gamma}{2} \left(\frac{\phi}{m_P} \right)^n \frac{3+Q}{1+7Q} \right). \quad (62)$$

Therefore, for both $n = 0, 2$ the dissipative ratio Q increases during inflation, and we can have the three kinds of scenarios: (a) 40-60 e-folds with weak dissipation only; (b) Starting in WDWI but ending inflation in SDWI; (c) 40-60 e-folds in the strong dissipative regime. On the other hand, T/H always increases for the logarithmic potential, so once the condition $T > H$ is fulfilled at the start of inflation the system will remain in the warm regime; for the quadratic potential it does so in WDWI with $Q < 1$, but once in SDWI this ratio decreases. For the slow-roll parameters, the ratio $\eta_\phi/(1+Q)$ in WDWI increases for $n = 0$, but it remains constant for $n = 2$, while in SDWI it decreases in both cases. Thus, in SDWI inflation will end either when the field reaches the critical value or by violating one of the conditions for low- T dissipation, whatever happens first.

The relation between Q and the vev of the inflaton field Eq. (25) is given by:

$$Q^{1/3}(1+Q)^2 \simeq \left(\frac{C_\phi}{3}\right)^{1/3} \left(\frac{C_\phi}{4C_R}\right) \left(\gamma\left(\frac{H}{m_P}\right)^{n-2}\right)^2 \left(\frac{\phi}{H}\right)^{2n-14/3}. \quad (63)$$

Notice that this relation, and therefore the different predictions, depends on γ through the combination $\tilde{\gamma} = \gamma(H/m_P)^{n-2}$, so we will use $\tilde{\gamma}$ as a model parameter in the following. For a quadratic potential this is just the ratio of the inflaton mass and the vacuum energy, $\tilde{\gamma} = \gamma = m_\phi^2 m_P^2 / V_0$, whereas for the logarithmic potential $\tilde{\gamma}$ is the ratio between the coupling constant $3\gamma = 3g^2 N_\chi / (8\pi^2)$ and the vacuum energy V_0 in Planck units. Using the relation Eq. (63) we have for the amplitude of the primordial spectrum during warm inflation:

$$P_{\mathcal{R}}^{1/2} \simeq \frac{1}{2\pi} \left(\frac{C_\phi}{4C_R}\right)^{1/2} \left(\frac{H}{\phi_*}\right) (1+Q_*)^{1/4}, \quad (64)$$

where we have left explicit the dependence on both H/ϕ_* and Q_* for simplicity. Indeed the spectrum only depends on one of these variables, say the value of the dissipative ratio at horizon crossing Q_* , and the model parameters C_ϕ and $\tilde{\gamma}$. The recipe now in order to get the parameter space available for warm inflation would be:

(a) For each pair of values $(\tilde{\gamma}, C_\phi)$, get the value of Q_* (ϕ_*) compatible with the observable value of primordial spectrum from Eq. (64).

(b) Check with Eqs. (59) and (60) whether one can obtain $Ne = 40 - 60$ e-folds of slow-roll inflation while having $T/H > 1$ and $\phi/T > 10$, and $\rho_R < V_0$. The radiation energy density during warm inflation is given by:

$$\frac{\rho_R}{V_0} = \frac{C_R}{9} \left(\frac{T}{H}\right)^4 \frac{V_0}{m_P^4}, \quad (65)$$

so that in principle it can be kept below V_0 by lowering the scale of the potential if needed.

(c) Check the predictions for the different observables: spectral index, running of the spectral index, tensor-to-scalar ratio.

The expressions for the spectral index and the running at leading order in the parameters are given in Table IV for the different regimes, including those for cold inflation for comparison. We stress that when $\gamma < 1$ in the warm inflationary regime, both weak and strong, the spectral index is blue tilted even for the logarithmic potential with a negative curvature of the potential. For small couplings, the spectral index would be blue-tilted in the weak dissipative regime whatever the dominant power in the potential at the time of horizon crossing, and it will only become red-tilted in the strong dissipative regime when $n > 6$. Nevertheless, for a large enough coupling the spectral index for

	$n_S - 1$		n'_S	
	$n = 0$	$n = 2$	$n = 0$	$n = 2$
CI	$-2\gamma \left(\frac{m_P}{\phi_*}\right)^2$	2γ	$-4\gamma^2 \left(\frac{m_P}{\phi_*}\right)^4$	$8\gamma^3 \left(\frac{\phi_*}{m_P}\right)^2$
WDWI	$\gamma(2-\gamma) \left(\frac{m_P}{\phi_*}\right)^2$	2γ	$4\gamma^2 \left(\frac{m_P}{\phi_*}\right)^4$	$2\gamma^2 \left(2 \left(\frac{\phi_*}{m_P}\right)^2 - Q_*\right)$
SDWI	$3(14-3\gamma) \frac{\gamma}{14Q_*} \left(\frac{m_P}{\phi_*}\right)^2$	$\frac{15\gamma}{7Q_*}$	$\frac{2\gamma^2}{7Q_*^2} \left(\frac{m_P}{\phi_*}\right)^4 \left(\frac{4}{Q_*} + 3\gamma - \frac{81}{28}\gamma^2\right)$	$-\frac{30\gamma^2}{49Q_*^2}$

TABLE IV: Predictions for the spectral index n_S and running of the spectral index n'_S , at leading order in γ , Q_* , ϕ_* , for the potentials given in Eqs. (56) and (57), for cold inflation (CI), weak dissipative warm inflation (WDWI), and strong dissipative warm inflation (SDWI).

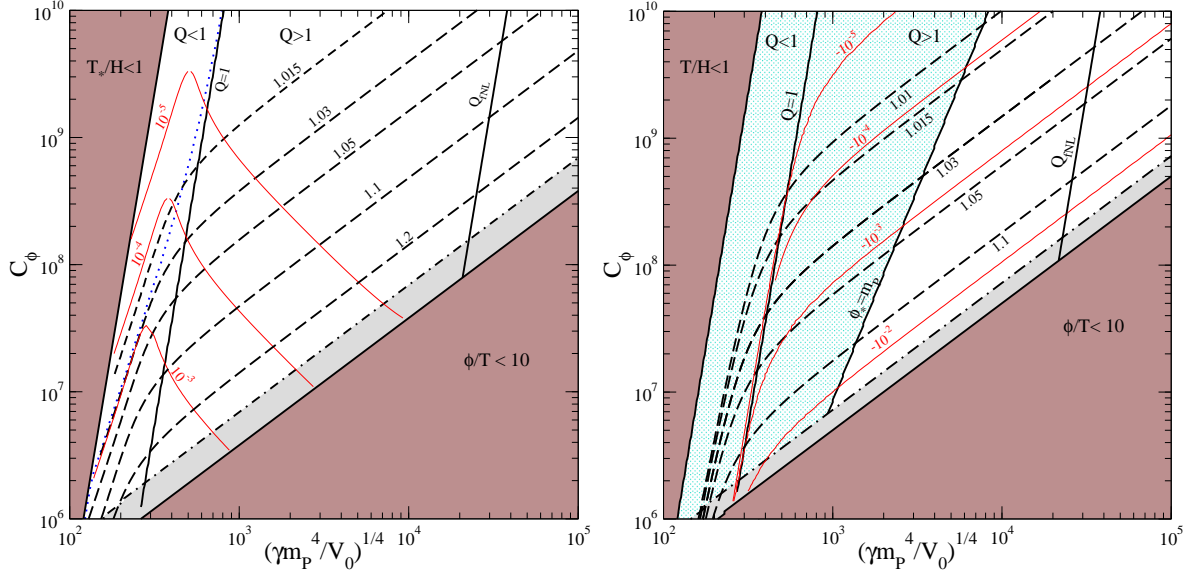


FIG. 3: The C_ϕ - $(\gamma m_P^4/V_0)^{1/4}$ plane for the logarithmic potential Eq. (57). Within the dark grey (brown) area we have $N_e < 40$ ($N_e < 0$ within the light grey area). To the right of the line $Q = 1$ we have strong dissipative warm inflation (SDWI), while to the left we have weak dissipative warm inflation (WDWI). Between the line $Q = 1$ and the dotted (blue) line inflation starts in WDWI but ends in SDWI. The dashed lines show the prediction for the spectral index, while the thin (red) lines that of the running of the spectral index. In the LHS plot we have taken $\gamma = 10^{-4}$, while in the RHS we have $\gamma = 2$. In the dotted area of the RHS plot, to the left of the line labelled $\phi_{**} = m_P$, the value of the inflaton field at horizon crossing is larger than m_P .

a logarithmic potential can be rendered red-tilted with $\gamma > 2$ in the weak dissipative regime, and $\gamma > 14/3$ in the strong dissipative regime. However, for the tensor-to-scalar ratio, taking into account Eqs. (63) and (64) we recover for warm inflation the same prediction as in cold inflation:

$$r \simeq \frac{2}{\pi^2 P_{\mathcal{R}}} \left(\frac{H}{m_P} \right)^2 \simeq 8.14 \times 10^{-3} \left(\frac{V_0^{1/4}}{10^{16} \text{ GeV}} \right)^4, \quad (66)$$

for any power n in the potential. Therefore for a scale of inflation $V_0 < 10^{16}$ GeV we have a negligible tensor contribution to the spectrum with $r < 0.01$.

In Fig. 3 we have plotted the parameter space available to get 40 (60) e-folds of warm inflation with a log potential, in the plane C_ϕ - $\tilde{\gamma}$, consistent with the observed amplitude of the primordial spectrum. On the LHS plot we have taken a small coupling with $\gamma = 10^{-4}$, while on the RHS plot we have $\gamma = 2$. Given that in this case during warm inflation the ratio T/H increases but ϕ/T decreases, the left shaded area is excluded because $T/H < 1$ at horizon crossing, while the right shaded area is excluded because we reach $\phi/T = 10$ before 40 e-folds after horizon crossing (60 e-folds for the light grey shaded area). This means that roughly the low- T dissipative regime ends, but still one could get some extra e-folds in the intermediate and high- T regime before inflation ends. The condition on ϕ/T only gives the most conservative upper limit on $\tilde{\gamma}$ for a given value of C_ϕ . On the other hand, for a logarithmic potential a small value of the coupling $\gamma = g^2 N_\chi / (8\pi^2)$, means that to fulfill the condition $m_\chi/T \gtrsim 10$ we need a larger value of the ratio ϕ/T . For example with $g \simeq 0.01$ one would have to impose $\phi/T \gtrsim 10^3$ instead, and the limit on C_ϕ increases approximately by a factor of 6 with respect to that shown in Fig. (3); similarly for $g \simeq 10^{-3}$ the limit increases approximately by a factor of 30.

In all the parameter space available, after 40 (60) e-folds the slow-roll conditions still hold, and the radiation energy density is still subdominant. That is, in order to end inflation we would have to tune the value of the field to the critical value in hybrid inflation. We included the predictions for the spectral index (dashed lines), and the running of the spectral index (thin solid lines). The spectrum is blue-tilted in both cases, and the stronger dissipation is, the closer the spectrum is to a scale invariant one. For a small coupling γ we have that the running is positive and goes like $n'_S \simeq 8(n_S - 1)^2 / (63Q_*)$. But by increasing the coupling we can reduce the tilt in the spectrum, and get a negative running, as shown on the RHS plot. By further increasing the coupling we could also revert the tilt of the spectrum. However a larger coupling implies a larger value of the inflaton vev at horizon crossing, and in the dotted area on the RHS plot we have $\phi > m_P$. As with cold inflation, with $\gamma > 1$ inflation is only viable in the weak dissipative regime for values $\phi > m_P$. But once in the strong dissipative regime, the extra friction helps in keeping

the value of the field subplanckian. The scale of inflation can be read from the value of $\tilde{\gamma}^{1/4} = (3\gamma m_P^4/V_0)^{1/4}$ for a given value of γ . And from Eqs. (63) and (64), we get the lines of constant Q_* in SDWI:

$$C_\phi \simeq 5.68 \times 10^{-13} Q_*^{-7/2} \tilde{\gamma}^2. \quad (67)$$

Taking into account the limit $Q_* < 1.3 \times 10^4$ for not having a too large deviation from gaussianity in the primordial spectrum, we have:

$$C_\phi \lesssim 2.27 \times 10^5 \left(\frac{\tilde{\gamma}^{1/4}}{10^4} \right)^8, \quad (68)$$

which gives the line “ Q_{fNL} ” in Fig. 3. We have also included in the plot the line $Q_* \simeq 1$ dividing the parameter space for WDWI and SDWI.

The predictions for a small coupling do not vary as far as $\gamma \lesssim 10^{-2}$, and they would be the same than in the LHS plot in Fig. (3). We can compare these with the ones obtained in supersymmetric cold hybrid inflation. For example for a value of the coupling between the inflaton and χ of the order $g \simeq 0.02/\sqrt{N_\chi}$ ($\gamma \simeq 5 \times 10^{-6}$) one gets a scale of inflation of the order $V_0^{1/4} \simeq 8.5 \times 10^{14}$ GeV, and a spectral index $n_S \simeq 0.98$ [43]. On the other hand in warm inflation, for the minimum allowed value of the dissipative parameter $C_\phi \simeq 10^6$ we have $\tilde{\gamma}^{1/4} = (3\gamma m_P^4/V_0)^{1/4} \simeq 200$ which gives a similar scale of inflation $V_0 \simeq 7.5 \times 10^{14}$ GeV for the same value of the coupling, but a spectral index $n_S \simeq 1.05$. Such a value for C_ϕ can be obtained for example by taking the Yukawa coupling h close to its perturbative value, $h \simeq \sqrt{4\pi}$, and the multiplicities of order of $N_\chi \simeq N_{decay} \simeq 100$. The minimum allowed value for $\tilde{\gamma}$ sets the maximum possible value for the scale of inflation in warm inflation. As long as this scale is below 10^{16} GeV, the tensor-to-scalar ratio is suppressed. Even when $\gamma \simeq 10^{-2}$ we have $\tilde{\gamma} \simeq 200$ and therefore $V_0^{1/4} \lesssim 10^{16}$ GeV. When $\gamma > 1$ by demanding $\phi < m_P$ the minimum value for $\tilde{\gamma}$ increases by an order of magnitude, so that again we have $V_0^{1/4} \lesssim 3 \times 10^{15}$, and therefore no tensor contributions.

As mentioned before, sugra corrections coming from the Kähler potential will contribute higher order terms in the potential, starting with a quartic term with minimal Kähler potential [41] $K(\Phi) = |\Phi|^2$:

$$V = V_0 \left(1 + \gamma \ln \frac{\phi}{m_P} + \frac{\phi^4}{8m_P^4} + \dots \right). \quad (69)$$

In CI, the quartic term starts to be non-negligible for a value of the coupling [43] $g \gtrsim 0.06/\sqrt{N_\chi}$ ($\gamma \simeq 4.6 \times 10^{-5}$), such that the curvature of the potential during inflation now becomes positive rendering the spectrum blue-tilted with

$$n_S - 1 \simeq 3 \left(\frac{\phi_*}{m_P} \right)^2 - 2\gamma \left(\frac{m_P}{\phi_*} \right)^2. \quad (70)$$

However, in warm inflation the addition of the sugra corrections works in the same direction as the radiative correction. Taking into account the quartic term in the slow-roll parameters, the spectral index is given by:

$$n_S - 1 \simeq \gamma \left(\frac{m_P}{\phi_*} \right)^2 (1 + \delta)(2 - \gamma(1 + \delta)), \quad (\text{WDWI}), \quad (71)$$

$$n_S - 1 \simeq \frac{3}{14Q_*} \gamma \left(\frac{m_P}{\phi_*} \right)^2 (14 - 3\gamma - 6(\gamma - 1)\delta), \quad (\text{SDWI}), \quad (72)$$

where

$$\delta = \frac{1}{2\gamma} \left(\frac{\phi_*}{m_P} \right)^4. \quad (73)$$

Then, in the small coupling regime $\gamma \ll 1$ sugra corrections make the coupling more blue-tilted, whereas in the large coupling regime with $\gamma > 14/3$ it would be more red-tilted, contrary to what happens in CI.

For the quadratic potential, Eq. (56) with $n = 2$, the allowed parameter space in the plane C_ϕ - γ ($\gamma = \eta_\phi$) compatible with the primordial spectrum is given in Fig. (4). Because now T/H and ϕ/T decrease during inflation, when varying C_ϕ and γ we have to check that we can get at least 40 (60) e-folds before $T/H < 1$ or $\phi/T < 10$. Indeed we always first reach $T = H$, and this corresponds to the shaded area on the LHS corner of the plot. In this case the low- T requirement $m_\chi/T \gtrsim 10$ is satisfied in general for $g \gtrsim 2 \times 10^{-3}$ ($g \gtrsim 10^{-4}$ for $C_\phi > 10^5$). On the other hand, when $\gamma \gg 1$ the constraint comes from having a small enough slow-roll parameter to start with at horizon crossing (the

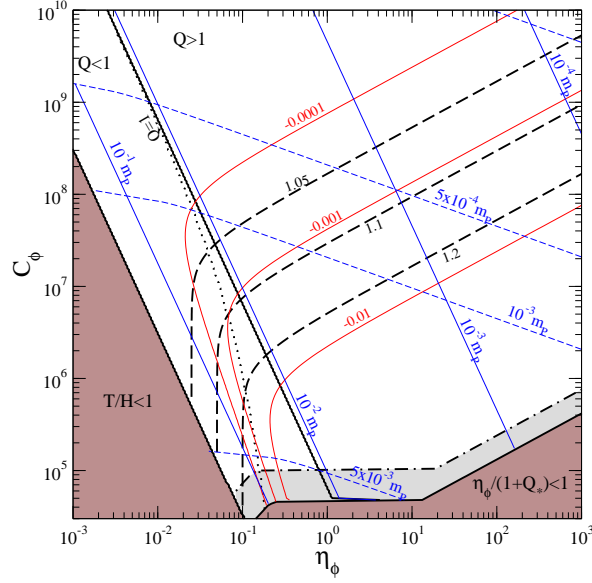


FIG. 4: The C_ϕ - η_ϕ plane for the quadratic potential, Eq. (56) with $n = 2$ and $\gamma = \eta_\phi$. Same conventions than in Fig. 3. The thin (blue) lines parallel to the line $Q = 1$ gives the upper bound on the scale of inflation $V_0^{1/4}$ demanding that $\rho_R < V_0$. The thin (blue) dashed lines are the upper limit from the constraint $\phi < m_P$.

bottom RHS corner). The lower limit on the dissipative parameter for having at least 40 e-folds of WDWI (SDWI) is $C_\phi \simeq 3 \times 10^4$ (5×10^4), which can be easily obtained with multiplicities of the order of 10-100. Given that T decreases, the radiation energy density never dominates during inflation, and in order to end inflation after the 40 (60) e-folds we would have to tune the value of the inflation field to the critical value. The spectral index (dashed lines) is always larger than 1, going like $n_S \simeq 1 + 2\gamma$ in WDWI (same than in cold inflation), but like $n_S \simeq 1 + 15\gamma/(7Q_*)$ in SDWI, i.e., it decreases by increasing C_ϕ for constant γ . The running of the spectral index is always negative (thin solid lines), in both regimes. In WDWI it is the contribution proportional to $\gamma^2 Q_*$ the dominant one (see Table IV). In SDWI we have at leading order $n'_S \simeq -2(n_S - 1)^2/15$. For example for $C_\phi \simeq 10^6$ and $\gamma \simeq 1$ we can have a large negative running $n'_S \simeq -0.01$, but with a rather large spectral index $n_S \simeq 1.27$, which seems excluded by the latest data. By increasing the dissipative parameter an order of magnitude, which could be accomplished by doubling the multiplicities, we can reach $n_S \simeq 1.1$ for $\gamma \simeq 1$, although with $n'_S \simeq -0.001$. The spectral index is still too blue-tilted, but within the allowed range by WMAP data [36].

The predictions related to the spectrum are rather insensitive to the value of V_0 . They depend on γ and Q_* , and the latter in turn depends on γ and C_ϕ . In particular, the lines of constant Q_* respectively in WDWI and SDWI are given by:

$$C_\phi \simeq 1.4 \times 10^4 Q_*^{1/3} \gamma^{-2}, \quad (\text{WDWI}), \quad (74)$$

$$C_\phi \simeq 1.4 \times 10^4 Q_*^{5/2} \gamma^{-2}, \quad (\text{SDWI}). \quad (75)$$

By varying the scale of inflation we just rescale the ratio ρ_R/V_0 at the start of inflation, the initial value of the field ϕ/m_P , and the prediction for the ratio r . Demanding that ρ_R does not dominate at least at horizon crossing gives us the maximum allowed value for each pair of values (C_ϕ, γ) , which in Fig. 4 is given by the thin (blue) lines parallel to the $Q = 1$ line. Well in WDWI, and SDWI, we have respectively:

$$V_0^{1/4} \simeq 1.26 Q_*^{-1/3} m_P, \quad (\text{WDWI}), \quad (76)$$

$$V_0^{1/4} \simeq 1.26 \times 10^{-2} Q_*^{-1/2} m_P, \quad (\text{SDWI}). \quad (77)$$

Then, the limit from non-gaussianity is approximately given in this case by the line $V_0^{1/4} \simeq 10^{-4} m_P$.

On the other hand, the dashed (blue) thin lines are the maximum value of the potential for having $\phi_* \leq m_P$, with $V_0^{1/4} \lesssim 0.16 m_P (C_\phi^3 \gamma)^{-1/10}$. By using the minimum C_ϕ value and γ read from the plot, the latter condition sets the upper bound for the potential at $V_0^{1/4} \simeq 1.2 \times 10^{16}$, which gives an upper bound on the tensor-to-scalar ratio, Eq. (66), $r \lesssim 0.017$. With respect to the inflaton mass, for example in WDWI with $C_\phi \simeq 10^6$ and $\gamma \simeq 0.05$ ($n_S \simeq 1.1$)

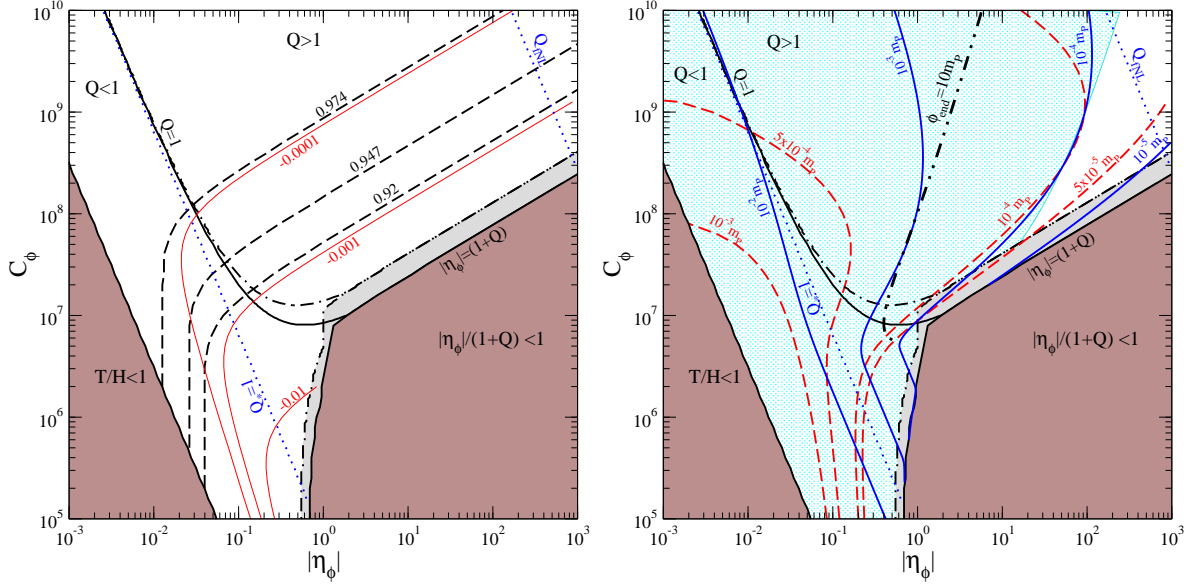


FIG. 5: The C_ϕ - $|\eta_\phi|$ plane for the hilltop potential, Eq. (56) with $n = 2$ and negative squared mass $\gamma = \eta_\phi < 0$. Same conventions than in Fig. 3. The curved thick solid (dot-dashed) line labelled $Q = 1$ to the left and by $|\eta_\phi| = (1 + Q)$ to the right separates WDWI from SDWI when $N_e = 40$ (60). The (blue) dotted line gives the value of Q_* at horizon crossing, with that labelled Q_{fNL} being the upper limit from non-gaussianity. On the LHS plot we have included the lines of constant n_S (dashed-lines) and n'_S (thin red solid lines). On the RHS plot the (blue) solid lines gives the the upper bound on the scale of inflation $V_0^{1/4}$ demanding that $\rho_R < V_0$ at least during 40 e-folds of inflation, while the (red) dashed lines are the corresponding value for having $\phi = m_P$ at the end of inflation. By setting $\rho_R = V_0$, in the dotted shaded area we have $\phi_{end} > m_P$, while to the left of the thick dot-dot-dashed line we have $\phi_{end} > 10m_P$.

we have the upper bound $V_0 \lesssim 7.2 \times 10^{15}$ GeV, which gives the upper bound on the inflaton mass $m_\phi \lesssim 1.2 \times 10^{12}$ GeV. On the other hand, in CI for the same value of γ , from the amplitude of the spectrum the scale of the potential is given by $V_0^{1/4} \simeq 4.8 \times 10^{14} g^{-1/2}$ GeV, and therefore $m_\phi \simeq 2.15 \times 10^{10} g^{-1}$ GeV, where g is the coupling between the inflaton and the X field. Having in CI similar values to those of WDWI for V_0 and m_ϕ requires a small value of the coupling $g \simeq 4 \times 10^{-3}$, whereas in warm inflation the predictions do not depend on this coupling as far as $g \gtrsim 2 \times 10^{-3}$.

V. HILLTOP MODELS

Hilltop models, or new inflation models, are given by the potential during inflation [4, 51]:

$$V = V_0 \left(1 - \frac{|\gamma|}{2} \left(\frac{\phi}{m_P} \right)^2 \right) + \dots, \quad (78)$$

where the dots account for higher order terms. This is no more than a quadratic potential of the kind considered in the previous section, but with a negative squared inflaton mass. In this model the inflaton starts at small values close to zero, and rolls off the top of the potential hill during inflation. When the field reaches a large enough value, higher order terms in the potential start contributing and inflation ends soon after. The mechanism for ending inflation differs from the quadratic hybrid model studied in the previous section, but for example the predictions for the spectral index, running and tensor-to-scalar ratio are the same replacing now γ with $-|\gamma|$. Thus, the primordial spectrum is red-tilted in both CI and WI, with a negative running (see Table IV). But given that the field now increases as inflation proceeds, during WI the dissipative ratio Q decreases instead, while T and the ratio ϕ/T keep increasing. In this case we can have either the 40(60) e-folds of inflation in WDWI or SDWI, or a transition from SDWI towards WDWI before the end of inflation. And once the system enters in the low- T regime, it remains there until the end of inflation.

Warm hilltop inflation has been studied in detail in Ref. [39], and in Fig. 5 we summarised the results. The analyses is done similarly to that of the potentials in the previous section. We show the values in the plane C_ϕ - $|\gamma|$

consistent with the amplitude of the primordial spectrum, which fix the initial conditions for warm inflation. The LHS shaded corner is excluded because $T \leq H$ at horizon crossing. The condition $m_\chi/T \gtrsim 10$ then only requires a coupling $g \gtrsim 10^{-4}$ for $C_\phi \gtrsim 10^5$. The RHS dark (light grey) shaded area is excluded because of the violation of the slow-roll condition before reaching $N_e = 40$ (60) e-folds. The lines of constant n_S and n'_S are given on the LHS plot. The solid line labelled $Q = 1$ divides the plane for WDWI (to the left) and SDWI (to the right). Therefore, in order to have at least 40 e-folds in SDWI it is required $C_\phi \gtrsim 10^7$. Nevertheless, the spectral index for such a value would be too red-tilted, but for example with $C_\phi \sim 10^8$ and $\gamma \sim 1$ we can have n_S within the 1σ range given in [36], $n_S = 0.96 \pm 0.013$.

As in the previous section, those predictions are independent of the scale of inflation, but by increasing the value of the height of the potential the radiation energy density also increases. Therefore, on the RHS plot the solid lines gives the upper limit on the scale of inflation such that the radiation does not dominate during inflation. For each point in the allowed plane, by setting V_0 to its upper bound we will end inflation after 40 e-folds, going smoothly from a vacuum dominated universe into a radiation dominated one. The line $V_0 = 10^{-2}m_P$ set the limit for not having a too large tensor-to-scalar contribution $r \lesssim 0.22$. We can also demand that inflation ends before the inflaton field reaches the Planck mass, and this gives the upper limit on $V_0^{1/4}$ shown by the dashed lines. The latter constraint is more restrictive than the one on the radiation energy density. Indeed, in the dotted shaded area on the RHS plot by keeping the value of V_0 such that $\rho_R = V_0$ after 40 e-folds we have that $\phi_{end} > m_P$. If we relax the condition on the inflaton vev, to the right of the dot-dot-dashed line the value of the inflaton field is still below $10m_P$.

VI. WARM INFLATION AND MODEL BUILDING

We have studied the parameter space that leads to a period of warm inflation in the low- T regime, for three kinds of generic single-field inflationary potentials. Implicitly, we are dealing with supersymmetric models for which the interactions relevant for the dissipative dynamics are given in Eq. (15), and the inflaton potential can be derived from Eq. (16). Supersymmetry ensures that quantum and thermal corrections to the effective potential are under control [27, 28]. On the other hand, the inflaton potential can be understood from the point of view of an effective field theory, with the inflationary potential dominated by the first few terms of a series, such that higher order terms are suppressed by the increasing inverse power of the cutoff scale. Without a specific setup to fix the cutoff, this naturally will be given by the Planck scale m_P . We have been considering models of inflation dominated by the first term of the expansion, but higher order terms appear naturally in supersymmetric models either by taking into account non-renormalizable interactions in the superpotential, and/or sugra corrections from the Kähler potential. The interactions in the superpotential can always be restricted by the use of symmetries, local, global or discrete. The pattern of interactions in Eq. (15) can follow for example by considering X and Y to be charged under some GUT group, but taking Φ to be a gauge singlet. We can further impose a discrete symmetry to select the leading term in the inflaton superpotential. During inflation the breaking of the discrete symmetry can lead to the formation of topological defects like domain walls [52], but these will be inflated away. For the standard superpotential for susy hybrid inflation, it is customary to impose a R -parity symmetry on the superpotential [44] in order to eliminate higher order terms for the inflaton apart from the linear term. But in general one can always expect non-renormalizable terms at some higher order in the potential, with generic couplings of the order of one. Such terms can be safely ignored in models where $\phi_{end} < m_P$, i.e., small field models.

Chaotic models do not fall into that category, and cold inflation is realised only for field values larger than m_P , with $\phi_* \simeq \sqrt{2N_e n} m_P$ and $\phi_{end} \sim m_P$. Once we have selected by the appropriate symmetry the power in the superpotential, we have to deal with sugra corrections from the Kähler potential. Just the simplest example, with a quadratic potential $W = M\Phi^2$ a minimal Kähler potential $K(\Phi) = |\Phi|^2$ induces higher order terms with

$$V \simeq M^2 |\Phi|^2 \left(1 + \frac{|\Phi|^6}{m_P^6} + \dots \right) \quad (79)$$

which invalidate slow-roll inflation. The choice of the Kähler potential compatible with inflation can be dictated again by imposing some symmetry [53], either for example a shift symmetry like in Refs. [54], or a Heisenberg symmetry used to ensure a flat enough potential [48]. In addition, the use of the Heisenberg symmetry implies the introduction of at least an extra degree of freedom, the modulus field. The presence of such fields, the moduli, is common in the low energy effective 4-dimensional sugra model derived from the compactification of the higher dimensional string theory. Although a suitable chaotic inflaton potential can be achieved by a specific choice of the Kähler potential [49], moduli fields need to be stabilised and fixed before hand in order to allow slow-roll inflation [55], which could be done at the expenses of some degree of fine-tuning in the potential. But see for example Ref. [56] for chaotic models derived in string theory with the higher order corrections under control.

Large field models, or chaotic models, are interesting because of the non-negligible prediction for the tensor-to-scalar ratio, $r \gtrsim 0.01$, within the range that could be detected by the current and future CMB experiments like Planck [38] and CMBPol [57]. And indeed, already the current limit on r disfavors quartic chaotic potentials and higher powers. On the other hand, in chaotic WI one predicts a smaller value for r , due to the suppression by T/H and the dissipative ratio Q , Eq. (37). Therefore, even only having WDWI, with $Q < 1$ at the time of horizon crossing, the suppression due to the temperature is enough to render the quartic (and sixth order) potential compatible with observations. This would happen for values of the dissipative parameter $C_\phi \simeq O(10^6)$, which as mentioned previously only requires multiplicities of the order of $O(100)$ or so for the fields. Still inflation takes place with values of the field $\phi > m_P$, and like in the CI scenario we have to deal with the problem of higher order corrections. By increasing the dissipative parameter by a couple of orders of magnitude, we are in SDWI with $Q \gg 1$, and the extra friction slows down enough the motion of the field for having inflation with a subplanckian inflaton vev. In this case higher order corrections can be easily kept under control⁴, and even the simplest model Eq. (79) gives rise to a viable model. Inflation ends when the slow-roll conditions Eq. (12) do not longer hold, similarly to cold inflation. But in this regime, the extra suppression due to the dissipative ratio gives a negligible prediction for the tensor-to-scalar ratio, as it would be expected from small-field models (i.e., subplanckian field models).

Hybrid models of the kind studied in Sect. II are small field models, with $\phi < m_P$ during inflation, and therefore one expects by definition to have a better control on the potential expansion. Nevertheless, when embedding the susy potential into the sugra framework, due to the constant term dominating the potential energy, sugra corrections generate a mass term for all scalars of the order of the Hubble parameter, and in particular for the inflaton field, the so-called “eta” problem [47]:

$$V_{sugra} \simeq e^{K(\Phi)}(V_0 + \dots) \simeq V_0 + \frac{V_0}{m_P^2} K_{\Phi\Phi^*} |\Phi|^2 + \dots \sim V_0 + cH^2 |\Phi|^2 + \dots, \quad (80)$$

where $K(\Phi)$ is the Kähler potential, and $K_{\Phi\Phi^*}$ the second derivative with respect to the inflaton field. Without tuning any parameter, one expects $|c| \simeq O(1)$, and then $|\eta_\phi| \sim O(1)$. Again, by taking into account some particular choice of superpotential + Kähler potential, like the standard susy hybrid inflation with minimal Kähler, different terms conspire to cancel out the quadratic term, although quartic and higher order terms will be present nonetheless. In this model the flat potential at tree-level is lifted by the 1-loop corrections giving rise to a log potential. However, quartic corrections become important for values of the coupling of the order of $g \simeq 0.06/\sqrt{N_\chi}$, rendering the spectrum too blue-tilted for larger values, and making $\phi_* > m_P$, so that we loose control on the corrections. Going beyond the minimal choice for K , the η problem is reintroduced, which requires as usual a mild tuning of the parameters to achieve inflation [58]; and working with effective sugra models coming from string compactifications the η problem is directly related to the moduli stabilisation problem [59]. Due to the coupling between modulus and inflaton through non-canonical kinetic terms, a small variation of the moduli field gives rise to a too large contribution to the η parameter, and a proper choice of the Kähler potential is mandatory in order to have inflation.

In a setup where we have dealt with moduli stabilisation, dissipation will help with the remaining η problem and higher order sugra corrections. When the inflationary dynamics is dominated by the log term, we can take larger values of the coupling $g > 0.06/\sqrt{N_\chi}$ ($\gamma > 4.6 \times 10^{-5}$) and still the quartic sugra corrections will be subdominant, with ϕ well below m_P . The value of the coupling at which the inflaton approaches m_P is larger, but still by decreasing accordingly the height of the potential, i.e., by increasing $\tilde{\gamma} = 3\gamma m_P^4/V_0$ we can keep the field within the range of the effective field description (see the RHS plot in Fig. 3). The main point is that we have more freedom to choose the value of the scale of inflation, not being directly fixed by the amplitude of the primordial spectrum due to its different thermal origin. In this case the constraint from $P_{\mathcal{R}}$ fixes the values at horizon crossing for the dissipative ratio Q_* and therefore the value of the inflaton field. Nevertheless, warm susy hybrid inflation predicts a blue-tilted spectrum, although the curvature of the potential is negative, in both regimes, weak and strong dissipation, except when the coupling is large enough such that the contributions from ϵ_ϕ are non negligible (see Table I). On the other hand, when sugra corrections generate a positive squared mass term for the inflaton field, we can have the scenario given in Fig. (4). Without the need of suppressing the mass, inflation can proceed in SDWI with $\gamma = \eta_\phi = m_\phi^2 m_P^2/V_0 > 1$. The spectrum is blue-tilted, but a large enough dissipative parameter can render it closer to a scale-invariant one. In this two hybrid examples, inflation ends when reaching the critical value ϕ_c . We will have to tune ϕ to such a value $N_e \sim 40 - 60$ e-folds after horizon crossing. But given the relative freedom we have now in choosing the height of the potential this does not impose a severe constraint to the model. Indirectly this is the same as in cold inflation, the amplitude of the spectrum fixes one of the parameters of the model, which in our case ends up being the critical

⁴ One would need to check how many terms in the potential expansion are relevant at the time of horizon crossing, and their impact on the inflationary predictions, but still they do not spoil the slow-roll conditions.

value of the field. Also the same as in CI, the tensor-to-scalar contribution is negligible, except in some corner of the parameter space for the log potential with the minimum allowed value for $\tilde{\gamma}$, for which we could get $r \simeq 0.01$.

When the quadratic sugra term gives rise to a negative squared mass term as the dominant term [60], we may have hilltop inflation, with the field starting near the top of the potential and evolving towards larger values. The problem in this case is how to end inflation without running into too large values of the inflaton field, i.e., by keeping $\phi < m_P$, which implies that the potential has to steepen sharply after N_e e-folds (see for example [61]). Nevertheless, CI hilltop models with the quadratic term seem to be disfavoured already by observations [62], and with a positive power it is required $n \gtrsim 3$. This again leaves open the question of how to suppress the lower terms when $\phi \ll m_P$ [63]. For WI, we have identified the parameter space that leads to enough inflation consistent with observations (see Fig. (5)), and even with a mass parameter $|\gamma| = |\eta_\phi| \simeq 1$ of the order expected in sugra theories, inflation in SDWI is a viable option. Although the problem still remains of how to end inflation with $\phi < m_P$. A nice solution would be to consider the model as an inverted hybrid model [64, 65], with the field rolling now from small values towards the critical value, and like in the standard hybrid model tune the value of $\phi_{end} = \phi_c$, with a low enough scale of inflation, below the GUT scale $V_0^{1/4} \lesssim 10^{16}$ GeV. For example the vacuum energy can originate from the F -term leading to susy breaking, with $V_0 \simeq m_{3/2}^2 m_P^2 \simeq (10^{11} \text{ GeV})^4$, with $m_{3/2} \sim 1$ TeV being the gravitino mass. On the other hand, during WI the radiation energy density increases, and inflation can end when $\rho_R \simeq V_0$, with a smooth transition from vacuum domination to a radiation dominated universe. The corresponding values of the vacuum energy required are given on the RHS plot in Fig. (5). However, typically we will have $\phi_{end} > m_P$ (dotted shaded area). In CI this kind of scenario could be implemented in the context of natural inflation [66], where the inflaton field is a pseudo Nambu-Goldstone boson (PNGB), with a periodic potential and a scale of spontaneous breaking $f > m_P$. The leading term in the expansion of the periodic potential leads to the negative quadratic term. In the context of warm inflation it would remain to be seen if such a field could couple to other fields in the model with the pattern of interactions required for the dissipative dynamics.

VII. SUMMARY AND FUTURE CHALLENGES

To summarize, we have revised the warm inflation dynamics, with the dissipative coefficient in the low- T regime derived in the close-to-equilibrium approximation [13] as computed in [16, 20]. Dissipation of the inflaton energy into light degrees of freedom follows from the two-stage mechanism in Ref. [14, 26, 27], with the interactions given in Eq. (15). For the inflationary potential we have focused on models where the primordial spectrum originates from the inflaton quantum fluctuations and the thermal fluctuations of the energy density dissipated. As particular models, we have studied supersymmetric models where the relevant inflationary potential is dominated by the first term in the expansion of the effective potential, but the analyses presented in Sect. II is rather general and it can be easily extended to other models. Chaotic models up to a power $n < 14$, and hybrid-like models with a logarithmic or a quadratic potential, always lead to a period of strong dissipation for a large enough dissipative coefficient. This facilitates the embedding of the models into a sugra framework as explained in Sect. VI. Apart from providing a solution to the standard η problem, this would open for example the possibility of having sugra inflation without fully stabilising the moduli fields, but just keeping them in a slow-roll trajectory. The large η_ϕ induced by the motion of the moduli can be counteracted by the dissipative dynamics.

Remarkable for chaotic models, even with weak dissipation, the different thermal origin of the primordial spectrum when compared to the cold inflation predictions render the tensor-to-scalar ratio consistent with observations for quartic models. On the contrary, hybrid models tend to give rise to a blue-tilted spectrum even when the curvature of the potential is negative. Reverting the sign of the quadratic term in hybrid models we revert the evolution of the inflation field from small to large values, the hilltop model, and the behavior of the dissipative parameter, with the tilt of the spectrum now being again red-tilted. Warm hilltop models when only considering one dominating term in the potential may end inflation with a too large value of the inflaton field. On the other hand, given the freedom we have now to choose the scale of inflation, not being directly dictated by the amplitude of the primordial spectrum, as an alternative this kind of models could be embedded without difficulty into an inverted hybrid model, where inflation ends when reaching the critical value as in the standard hybrid case.

A feature generally found of warm inflation models so far has been the requirement of many fields, usually in the hundreds or more. This is in contrast to cold inflation models which usually involve just a few fields. In the high energy regime, most particle physics models exhibit a large proliferation of fields, with the ultimate example being that of string theory, where field numbers can become huge. Thus warm inflation models possibly have a natural setting at high energy, based on what model building has found out about field content of particle physics models at high energy scales. Some studies have been made of warm inflation models in the context of string theory [67] (a variation of the warm inflation picture in string models also has been explored [68]), and further analysis may prove interesting.

The results presented here assume that the relevant N_e e-folds of inflation take place in the low- T regime, such that the equations of motion can be solved analytically. In the intermediate or high T regime, with $m_\chi \gtrsim T$, the dependence of the dissipative coefficient Υ changes, for example with $\Upsilon \propto T \ln T$ ($m_\chi \ll T$), or $\Upsilon \propto T^{-1} \ln T$ ($m_\chi \ll hT$) [13, 16, 20], but still with this T dependence we could have some extra e-folds of inflation, and taking into account this regime can enhance the parameter space for warm inflation. For example for monomials potentials this would happen at the end of inflation, and having a smaller no. of e-folds in the low- T regime means that horizon crossing may take place in SDWI for smaller values of the dissipative parameter C_ϕ , which implies a smaller prediction for the tensor-to-scalar ratio. On the contrary, for hilltop models as those in Sect. V, the intermediate/high T regime will occur at the beginning of inflation. This opens up the possibility of having horizon crossing in that regime, and different predictions for the spectral index, running, and tensor-to-scalar ratio than those given in Sect. IV.

On the other hand going beyond the low- T approximation one would have to take into account the thermal corrections to the inflaton effective potential, which we have neglected so far. With the two-stage mechanism for dissipation, those are due to the contribution of the self energies of the heavy fields χ and ψ_χ , which in turn receive thermal corrections due to the interaction with the light fields (the thermal bath) y and ψ_y [28]. In a hybrid model where inflation ends by a phase transition once $m_{\chi_R}^2 < 0$, the thermal corrections will tend to keep this squared mass positive and delay the phase transition. All effects considered, they tend to increase the duration of inflation, and it remains to be seen how this will affect the time of horizon crossing and the primordial spectrum.

Acknowledgements

The work of M.B.G. is partially supported by the M.E.C. under contract FIS 2007-63364 and by the ‘‘Junta de Andaluc a’’ group FQM 101. A.B. is supported by STFC.

-
- [1] A. H. Guth, Phys. Rev. D **23** (1981) 347.
 - [2] K. Sato, Phys. Lett. B **99** (1981) 66.
 - [3] A. Albrecht and P. J. Steinhardt, Phys. Rev. Lett. **48** (1982) 1220.
 - [4] A. D. Linde, Phys. Lett. B **108** (1982) 389.
 - [5] A. D. Linde, Phys. Lett. B **129** (1983) 177.
 - [6] A. Berera, Phys. Rev. Lett. **75**, 3218 (1995).
 - [7] L. Z. Fang, Phys. Lett. B **95**, 154 (1980).
 - [8] I. G. Moss, Phys. Lett. B **154**, 120 (1985).
 - [9] J. Yokoyama and K. I. Maeda, Phys. Lett. B **207**, 31 (1988).
 - [10] A. Berera and L. Z. Fang, Phys. Rev. Lett. **74**, 1912 (1995).
 - [11] A. Berera, Nucl. Phys. B **585**, 666 (2000).
 - [12] A. Berera, Phys. Rev. D **54**, 2519 (1996).
 - [13] A. Berera, M. Gleiser and R. O. Ramos, Phys. Rev. **D58**, 123508 (1998).
 - [14] A. Berera and R. O. Ramos, Phys. Rev. D **63**, 103509 (2001).
 - [15] J. Yokoyama and A. D. Linde, Phys. Rev. D **60**, 083509 (1999).
 - [16] I. G. Moss, C. Xiong, arXiv:hep-ph/0603266.
 - [17] A. Berera, M. Gleiser and R. O. Ramos, Phys. Rev. Lett. **83**, 264 (1999).
 - [18] M. Bastero-Gil and A. Berera, Phys. Rev. D **76**, 043515 (2007).
 - [19] A. Berera, Contemp. Phys. **47**, 33 (2006).
 - [20] A. Berera, I. G. Moss and R. O. Ramos, In Press Reports on Progress in Physics arXiv:0808.1855 [hep-ph].
 - [21] A. Berera, Phys. Rev. D **55**, 3346 (1997).
 - [22] A. N. Taylor and A. Berera, Phys. Rev. **D62**, 083517 (2000).
 - [23] L. M. H. Hall, I. G. Moss and A. Berera, Phys. Rev. **D69**, 083525 (2004).
 - [24] I. G. Moss and C. Xiong, JCAP **0811**, 023 (2008).
 - [25] H. P. de Oliveira and R. O. Ramos, Phys. Rev. **D57**, 741 (1998); E. Gunzig, R. Maartens, and A. V. Nesteruk, Class. Quant. Grav. **15**, 923 (1998); M. Bellini, Phys. Rev. **D58**, 103518 (1998); M. Bellini, Nucl. Phys. **563**, 245 (1999); W. Lee and L. Z. Fang, Phys. Rev. **D59**, 083503 (1999); J. M. F. Maia, and J. A. S. Lima, Phys. Rev. **D60**, 101301 (1999); A. P. Billyard and A. A. Coley, Phys. Rev. D **61**, 083503 (2000); H. P. de Oliveira and S. E. Joras, Phys. Rev. **D64**, 063513 (2001); I. Dymnikova and M. Khlopov, Eur. Phys. J. C **20**, 139 (2001); L. P. Chimento, A. S. Jakubi, N. A. Zuccala, and D. Pavon, Phys. Rev. **D65**, 083510 (2002); H. P. De Oliveira, Phys. Lett. B **526**, 1 (2002); R. H. Brandenberger and Y. Yamaguchi, Phys. Rev. D **68**, 023505 (2003); R. Jeannerot and M. Postma, JHEP **0505**, 071 (2005); J. P. Mimoso, A. Nunes and D. Pavon, Phys. Rev. D **73**, 023502 (2006); S. del Campo and R. Herrera, Phys. Lett. **B653**, 122 (2007); L. M. H. Hall and H. V. Peiris, JCAP **0801**, 027 (2008); S. Mohanty and A. Nautiyal, arXiv:0807.0317 [hep-ph].
 - [26] A. Berera and R. O. Ramos, Phys. Lett. **B567**, 294 (2003).

- [27] A. Berera and R. O. Ramos, Phys. Rev. D **71**, 023513 (2005); Phys. Lett. B **607**, 1 (2005).
- [28] L. M. H. Hall and I. G. Moss, Phys. Rev. D **71**, 023514 (2005).
- [29] A. Berera, I. G. Moss and R. O. Ramos, Phys. Rev. D **76**, 083520 (2007).
- [30] I. G. Moss and C. Graham, Phys. Rev. D **78**, 123526 (2008).
- [31] S. Gupta, A. Berera, F. F. Heavens and S. Matarrese, Phys. Rev. D **66**, 043510 (2002).
- [32] B. Chen, Y. Wang and W. Xue, JCAP **0805**, 014 (2008).
- [33] I. G. Moss and C. Xiong, JCAP **0704**, 007 (2007).
- [34] D. S. Salopek and J. R. Bond, Phys. Rev. D **42**, 3936 (1990); T. Falk, R. Rangarajan and M. Srednicki, ApJ **403**, L1 (1993); A. Gangui et al., ApJ **430**, 447 (1994).
- [35] J. M. Maldacena JHEP **05**, 013 (2003); V. Acquaviva et al., Nucl. Phys. B **667**, 119 (2003); G. I. Rigopoulos, E. P. S. Shellard and B. J. W. van Tent, Phys. Rev. D **72**, 083507 (2005).
- [36] E. Komatsu et al., arXiv:0803.0547 [astro-ph].
- [37] A. P. S. Yadav and B. D. Wandelt, Phys. Rev. Lett **100**, 181301 (2008).
- [38] Planck Surveyor Mission: <http://www.rssd.esa.int/Planck>.
- [39] J. C. Bueno Sanchez, M. Bastero-Gil, A. Berera and K. Dimopoulos, Phys. Rev. D **77**, 123527 (2008).
- [40] W. H. Kinney, E. W. Kolb, A. Melchiorri and A. Riotto, Phys. Rev. D **78**, 087302 (2008).
- [41] C. Panagiotakopoulos, Phys. Rev. D **55**, 7335 (1997); A. Linde and A. Riotto, Phys. Rev. D **56**, R1841 (1997).
- [42] W. Buchmuller, L. Covi and D. Delepine, Phys. Lett. B **491**, 183 (2000); M. Kawasaki, M. Yamaguchi and J. Yokoyama, Phys. Rev. D **68**, 023508 (2003).
- [43] V. N. Senoguz and Q. Shafi, Phys. Lett. B **567**, 79 (2003).
- [44] G. R. Dvali, Q. Shafi and R. K. Schaefer, Phys. Rev. Lett. **73** (1994) 1886; Phys. Lett. B **567** (2003) 79.
- [45] A. D. Linde, Phys. Lett. B **259**, 38 (1991).
- [46] E. J. Copeland, A. R. Liddle, D. H. Lyth, E. D. Stewart and D. Wands, Phys. Rev. D **49**, 6410 (1994).
- [47] M. Dine, L. Randall and S. Thomas, Phys. Rev. Lett. **75**, 398 (1995).
- [48] E. D. Stewart, Phys. Rev. D **51**, 6847 (1995); M. K. Gaillard, H. Murayama and K. A. Olive, Phys. Lett. B **355**, 71 (1995); M. K. Gaillard, D. H. Lyth and H. Murayama, Phys. Rev. D **58**, 123505 (1998).
- [49] H. Murayama, H. Suzuki, T. Yanagida and J. Yokoyama, Phys. Rev. D **50**, 2356 (1994).
- [50] P. Binetruy and G. R. Dvali, Phys. Lett. B **388**, 241 (1996); E. Halyo, Phys. Lett. B **387**, 43 (1996); C. F. Kolda and J. March-Russell, Phys. Rev. D **60**, 023504 (1999).
- [51] L. Boubeker and D. H. Lyth, JCAP **0507**, 010 (2005); K. Kohri, C. M. Lin and D. H. Lyth, JCAP **0712**, 004 (2007).
- [52] Y. Zel'dovich, I. Kobzarev and L. Okun, Sov. Phys. JETP **40**, 1 (1975); T. Kibble, J. Phys **A9**, 1387 (1976); A. Vilenkin, Phys. Rep. **121**, 263 (1985); S. A. Abel, S. Sarkar and P. L. White, Nucl. Phys. B **454**, 663 (1995).
- [53] A. B. Goncharov and A. D. Linde, Phys. Lett. B **139**, 27 (1984).
- [54] M. Kawasaki, M. Yamaguchi and T. Yanagida, Phys. Rev. Lett. **85**, 3572 (2000); M. Yamaguchi and J. Yokoyama, Phys. Rev. D **63**, 043506 (2001); P. Brax and J. Martin, Phys. Rev. D **72**, 023518 (2005).
- [55] J. R. Ellis, Z. Lalak, S. Pokorski and K. Turzynski, "The price of WMAP inflation in supergravity," JCAP **0610**, 005 (2006); S. C. Davis and M. Postma, JCAP **0803**, 015 (2008); L. Covi, M. Gomez-Reino, C. Gross, J. Louis, G. A. Palma and C. A. Scrucca, JHEP **0808**, 055 (2008).
- [56] E. Silverstein and A. Westphal, Phys. Rev. D **78**, 106003 (2008); L. McAllister, E. Silverstein and A. Westphal, arXiv:0808.0706 [hep-th]; N. Kaloper and L. Sorbo, arXiv:0811.1989 [hep-th].
- [57] D. Baumann et al., arXiv:0811.3919 [astro-ph].
- [58] M. Bastero-Gil, S. F. King and Q. Shafi, Phys. Lett. B **651**, 345 (2007); O. Seto and J. Yokoyama, Phys. Rev. D **73**, 023508 (2006); C. M. Lin and J. McDonald, Phys. Rev. D **74**, 063510 (2006).
- [59] P. Brax, C. van de Bruck, A. C. Davis and S. C. Davis, JCAP **0609**, 012 (2006); S. C. Davis and M. Postma, JCAP **0804**, 022 (2008).
- [60] K. I. Izawa and T. Yanagida, Phys. Lett. B **393**, 331 (1997); I. Izawa, M. Kawasaki and T. Yanagida, Phys. Lett. B **411**, 249 (1997).
- [61] M. Dine and A. Riotto, Phys. Rev. Lett. **79**, 2632 (1997); G. German, G. G. Ross and S. Sarkar, Nucl. Phys. B **608**, 423 (2001); N. Arkani-Hamed, H. C. Cheng, P. Creminelli and L. Randall, JCAP **0307**, 003 (2003).
- [62] L. Alabidi and D. H. Lyth, JCAP **0605**, 016 (2006) 016; JCAP **0608**, 013 (2006); L. Alabidi and J. E. Lidsey, arXiv:0807.2181 [astro-ph].
- [63] G. G. Ross and S. Sarkar, Nucl. Phys. B **461**, 597 (1996).
- [64] D. H. Lyth and E. D. Stewart, Phys. Rev. D **54**, 7186 (1996); S. King and J. Sanderson, Phys. Lett. B **412**, 19 (1997).
- [65] M. Bastero-Gil and S. F. King, Phys. Lett. B **423**, 27 (1998).
- [66] K. Freese, J. A. Fireman and A. V. Olinto, Phys. Rev. Lett **65**, 3233 (1990); F. C. Adams, J. R. Bond, K. Freese, J. A. Frieman and A. V. Olinto, Phys. Rev. D **47**, 426 (1993).
- [67] A. Berera and T. W. Kephart, Phys. Rev. Lett. **83**, 1084 (1999); Phys. Lett. B **456**, 135 (1999).
- [68] D. Battfeld, T. Battfeld and A. C. Davis, JCAP **0810**, 032 (2008); D. Battfeld and T. Battfeld, arXiv:0812.0367 [hep-th].